Forest Ecology and Management 500 (2021) 119652

Contents lists available at ScienceDirect

Forest Ecology and Management

journal homepage: www.elsevier.com/locate/foreco

Logging Amazon forest increased the severity and spread of fires during the 2015–2016 El Niño

Paulo Eduardo Barni [a,*], Anelícia Cleide Martins Rego [a], Francisco das Chagas Ferreira Silva [a], Richard Anderson Silva Lopes [b], Haron Abrahim Magalhães Xaud [c], Maristela Ramalho Xaud [c], Reinaldo Imbrozio Barbosa [d], Philip Martin Fearnside [e,f]

[a] Universidade Estadual de Roraima – UERR, Campus Rorainópolis, Av. Senador Hélio Campos, s/nº, 69375-000 Rorainópolis, Roraima, Brazil
[b] Corpo de Bombeiros Militares de Roraima, Coordenação Estadual de Proteção e Defesa Civil, Avenida Venezuela, 1271, 69309690 Boa Vista, Roraima, Brazil
[c] Empresa Brasileira de Pesquisa Agropecuária – Embrapa/RR, Rodovia BR 174, Km 8, Distrito Industrial, 69301-970 Boa Vista, Roraima, Brazil
[d] Instituto Nacional de Pesquisas da Amazônia (INPA), Rua Coronel Pinto, 315, 69301-150 Boa Vista, Roraima, Brazil
[e] Instituto Nacional de Pesquisas da Amazônia (INPA), Av. André Araújo, 2936, 69067-375 Manaus, Amazonas, Brazil
[f] Brazilian Research Network on Global Climate Change – Rede Clima, Av. dos Astronautas, 1758 - Jardim da Granja, São José dos Campos – SP 12227-010, Brazil

ARTICLE INFO

Keywords:
Environmental modeling
Land use
Land cover
Remote sensing
Amazon

ABSTRACT

Forest fires degrade Amazon forest and its natural functions. Logging, deforestation and the increased frequency of prolonged droughts have contributed to the high recurrence of forest fires in the Amazon. Fires have impacted areas that, until recently, were considered immune to fire, such as the southern portion of the Brazilian state of Roraima, which is characterized by forest types that occur in environments with high natural humidity but that are now strongly impacted by selective logging (SL). The objective of this study was to determine the severity and spread of fire in the forests of southern Roraima, taking as a reference the great forest fire that occurred during the 2015–2016 El Niño. We mapped fire scars and forest biomass from remote sensing and data from forest inventories in a 6657.3 km^2 study area, of which 6512.4 km^2 (97.8%) had originally been forest and 5412.3 km^2 (81.3%) was still forest in 2016. The 2015/2016 fires affected an estimated at 682.2 km^2, or 12.6% of the area that was still forest in 2016. Vulnerability maps of the forest were made using the weights-of-evidence method. The biomass impacted by fire totaled 26.4 $\times$ 10^6 Mg, representing 9.5% of the total mapped for the study area (277.4 $\times$ 10^6 Mg). The biomass killed by the fire totaled 5.9 $\times$ 10^6 Mg, representing 22.3% of the biomass affected by the fires. The highest level of fire severity (very strong) proportionally affected 84.6% more forest biomass inside than outside SL areas. Forest vulnerability to fires increased by 265.5% in terms of area and by 400.7% in terms of biomass when exposed to SL. Logging also increased the severity of fires when they occurred: a hectare of burned forest was 85.9% more likely to have a "very strong" fire if it had been previously logged, and burned areas that had been logged lost, on average, 2.9% more of their pre-fire biomass to the fire than those that had not been logged (86.5 Mg ha^{-1} versus 84.0 Mg ha^{-1}). Considering only the ombrophilous forest, the mean biomass of forest that was logged and burned was 310.7 Mg ha^{-1}, or 30.8% lower than the mean biomass of 448.7 Mg ha^{-1} in logged but unburned areas, showing a substantial biomass loss to fire (average of 138.0 Mg ha^{-1}). SL more than doubled the impact of fire on biomass loss as compared to the impact of the logging itself. In addition to its contribution to carbon emissions and other impacts, the amplifying effect of SL on forest fires indicates that the assumption that authorized forest management projects in Amazonia are sustainable is unwarranted. The future role of this practice should be rethought, existing projects should be subject to close inspection and control, and unauthorized logging should be identified and repressed. The policy of allowing sale of wood from clearcutting projects should be rethought because it provides a loophole for laundering wood from illegal logging.

* Corresponding author.
E-mail addresses: pbarni@uerr.edu.br (P.E. Barni), anelycia.com@gmail.com (A.C.M. Rego), chagasferreirasilva@gmail.com (F.C.F. Silva), raslopes@gmail.com (R.A.S. Lopes), haronxaud@gmail.com (H.A.M. Xaud), marisxaud@gmail.com (M.R. Xaud), reinaldo@inpa.gov.br (R.I. Barbosa), pmfearn@inpa.gov.br (P.M. Fearnside).

https://doi.org/10.1016/j.foreco.2021.119652
Received 30 March 2021; Received in revised form 17 August 2021; Accepted 22 August 2021
Available online 10 September 2021

1. Introduction

Forest fires are a threat to the integrity and biodiversity of forests (McLauchlan et al., 2020), and to the Amazon forest's carbon storage and hydrological cycling functions (da Silva et al., 2018; Fearnside, 2008; Fearnside et al., 2013; Rappaport et al., 2018; Ziccardi et al., 2019). The ignition sources of forest fires in the Amazon are the result of human actions, such as burning in nearby newly cleared forest or for pasture maintenance or for slash-and-burn family farming, while selective logging (SL) plays an important role in making the forest vulnerable to the entry and propagation of fire (Alencar et al., 2006; Aragão and Shimabukuro, 2010; Berenguer et al., 2014; Brando et al., 2014, 2019; Uhl and Buschbacher, 1985; Xaud et al., 2013). SL has been indicated as one of the factors for the spread of forest fires even in places that are distant from the main foci of deforestation (Alencar et al., 2015; Broadbent et al., 2008; Hethcoat et al., 2020; Silva et al., 2018).

Prolonged drought events driven by the increasing frequency of severe El Niño events have a direct effect on the spread of forest fires in the Amazon (Aragão et al., 2018; Jiménez-Muñhoz et al., 2016; Meira-Junior et al., 2020; Nepstad et al., 2004, 2007), as do the effects of changes in land use and cover and predatory logging (Brando et al., 2014, 2019). The frequency of forest fires has increased in areas that (until recently) were considered immune to fire due to the natural humidity of the forest; however, the factors that attenuate or amplify fire occurrence are still little studied (Barni et al., 2015a; da Silva et al., 2018; Fonseca et al., 2017; Turubanova et al., 2018).

The Amazon provides essential environmental services (e.g., Fearnside, 2008), and conserving these requires understanding of the interactions between climatic phenomena and human activities and their effects on the degradation of forest biomass. Systematic mapping is one of the remote-sensing tools of great importance for the understanding the spatial distribution and the spreading behavior of forest fires and it is an intelligent way to provide input for the improvement of public policies to combat the indiscriminate use of fire. Systematic mapping can provide estimates of greenhouse-gas (GHG) emissions on a large scale and contribute to improving the calculations representing biomass and carbon affected by fire and deforestation (Aragão et al., 2018; Baccini et al., 2012). Brazil's current National Inventory of GHG Emissions (Brazil, MCTI, 2020) does not consider emissions from understory forest fires when calculating emissions from land-use change and forestry. This fact persists, in part, due to the small volume of work carried out in this area of knowledge and the large uncertainties involved in calculating the emission factors.

Several spectral indices have been developed or adapted to improve the mapping of burned areas: NDVI, SAVI, EVI, EVI2, GEMI, BAI, BAIM, NBR, NBR2, CSI and MIRBI (Bastarrika et al., 2011; Chuvieco et al., 2002; Stropianna et al., 2012). New approaches based on spectral mixture analysis (SMA) and image fractions (Quintano et al., 2006) are useful for mapping burned areas. Canopy damage by selective logging and fire, including their severity (capacity to damage the forest), have been successfully mapped using the Normalized Difference Fraction Index (NDFI) (Souza Jr. et al., 2005a, 2005b, 2013).

Halting or greatly reducing deforestation would clearly have a substantial benefit in avoiding forest fires because the burning of felled trees in newly cleared areas is a major source of ignition for fire in adjacent forests. Note that the forest is not intentionally set on fire, but rather fire escapes from nearby areas that are being burned either as part of the initial clearing or in subsequent management of the agricultural and ranching systems.

One of the great challenges we currently face is a better understanding of the relationship between deforestation behavior and the application of efficient public policies (West and Fearnside, 2021). Policies are also needed to help change the practices used in agriculture and ranching (which today are still based on fire) to the use of technologies that allow the incorporation into the soil of the biomass of second growth cut to prepare forest for planting and in the maintenance of pastures free of invading woody vegetation. However, implementation of these systems has proved to be difficult in the Amazon because these alternatives to fire demand increased production costs.

In the southern portion of Brazil's state of Roraima (in northern Amazonia), deforestation is strongly stimulated by both legal and illegal logging (Barni et al., 2020; Condé et al., 2019). In this region, authorizations to use wood from areas being deforested in projects licensed for clearcutting by Roraima's State Foundation for the Environment and Water Resources (FEMARH) provide the documentation for most of the "legal" logs delivered to sawmills. However, much of the wood that theoretically comes from the areas approved for clearcutting or for forest management does not actually come from these areas, but rather from selective logging in forests that are not authorized for either activity. For example, based on a questionnaire applied to 38% of the sawmills in Rorainópolis in 2013, Crivelli et al. (2017) reported that 54% of the wood volume came from deforestation projects, 11% from forest-management projects, and for 35% of the wood the sawmill owners were "unable to specify" the source.

The great majority of requests to FEMARH from landowners for deforestation authorizations are merely a means to legalize the sale of timber, rather than for the stated purpose of clearing land for agriculture and pasture. This is clearly shown by the fact that the 12,480.9 ha of deforestation authorized by FEMARH in southern Roraima between 2010 and 2015, only 26.2% was actually deforested, as shown by our mapping based on data from INPE's PRODES program (Brazil, INPE, 2020). If the authorized areas are, in fact, deforested, they are logged before the deforestation is done; if these areas are not in fact deforested, the logging is done, and the unharvested trees are left standing. The volume harvested in the authorized areas is less than the authorized amount. It is reasonable to suppose that this is because, given the lack of inspections, it is more profitable for the loggers to cut trees of the most-valuable species in a wider area of forest than it is to harvest the permitted volume only within the authorized area, where part of the harvest would be composed of less-valuable species.

In January 2021 the municipality (county) of Rorainópolis (in southern Roraima) was added to the federal "blacklist" of priority locations for actions to prevent, monitor and control deforestation in the Amazon (Oliveira, 2021). Logging in this area has only minimal control, and, due to insufficient staff, FEMARH, does not make field inspections to verify that the specified limits and procedures are respected. The lack of inspections at the sites undergoing logging or deforestation does not mean that all parts of the production chain are free of influence from regulations. The federal environmental agency (the Brazilian Institute for the Environment and Renewable Natural Resources, or IBAMA) occasionally inspects sawmills to see if the amount of wood present is compatible with the documentation. In 2018 such an inspection in Rorainópolis found that virtually none of the sawmills were in compliance, and the sawmills were shut down (G1, 2018a). Note that 2018 was after the 2015–2016 El Niño fires that are the subject of the current study and was before the Jair Bolsonaro presidential administration began in January 2019, with a notable relaxation of environmental controls and gutting of IBAMA (see Ferrante and Fearnside, 2019).

Logging is not done by the owners of the land, but instead is done either by logging teams working for sawmills or by independent loggers who pay a landowner to allow the timber to be harvested and sold to sawmills. There is clearly no motivation for sustainability, and those doing the logging may also invade adjacent properties or government land to remove additional timber. Inspection is limited to visits to sawmills to check if the volume of stockpiled wood is compatible with the maximum amounts specified in the licenses. Logging trucks are occasionally stopped by IBAMA to check the permit for transporting timber (the "document of forest origin," or DOF), but if a truck is not stopped the transport permit is often reused multiple times (Barni and Silva, 2017).

Throughout Brazilian Amazonia the permits issued for transporting timber from authorized forest-management projects are frequently used

in the same way as those for deforestation projects, with the volume for which the permits are issued coming, in reality, from logging in other areas, including indigenous lands and other protected areas where logging is forbidden (Brancalion et al., 2018). Regardless of any official authorization for "sustainable" forest management in rural properties in our study area, the actual implementation of such practices was "null or incipient" at the time of our study (Gimenez et al., 2015).

The present case study aims to determine the effects of SL on the severity and spread of understory fire in southern Roraima considering the mega forest fire that occurred in this part of the Amazon during the El Niño event of 2015–2016 (Fonseca et al., 2017). Areas "affected" by forest fire are areas where an understory fire occurred during the 2015–2016 El Niño as indicated by burned litter and charring at the base of trees. Our hypothesis is that SL favored an increase in the severity of fire and its spread (increased area affected by fire, both by the increased sizes of the fire scars and by increased number of scars) both within the logged areas and in neighboring unlogged areas, contributing to greater exposure of forest biomass to fire. The specific questions the study addresses are: (i) What was the extent of the area affected by fires and the amount of forest biomass lost in the study area considering four levels of fire severity? (ii) What was the proportional contribution of SL in spreading the fire? (iii) What was the area of the exposed forest and what was the magnitude of forest biomass vulnerable to new forest fires in the study area?

To answer question (i) we used a geographic information system (GIS) and geoprocessing tools, combined with inventory data, to assess the loss of forest biomass at four levels of fire severity as defined by Fernandes-Manso et al. (2016) in areas with signs of SL and in areas without signs of SL. To answer questions (ii) and (iii) we used the weights-of-evidence method (Barni et al., 2015b, 2020; Soares-Filho et al., 2006; Leite-Filho et al., 2021). Maps of weights-of-evidence have the ability to capture the influence of variables that are spatially related to the occurrence of forest fire (Silvestrini et al., 2011).

Our study will provide improvements for understanding the relationship between the severity of fire and previous disturbance by SL. Among the uses for this information is improvement of carbon-emission calculations due to forest degradation in the Amazon (e.g., Brazil, MCTI, 2020).

2. Materials and methods

2.1. Study area

The study area is located in the southern portion of the state of Roraima, covering the areas that include the seat of the municipality (county) of Rorainópolis and the towns (*vilas*) of Colina and Equador. The area also includes small parts of the municipalities of Caracaraí (90.5 km^2, 1.4% of the study area) and São Luiz (164.2 km^2, 2.5%) (Table S1 in the Supplementary Material). The area includes 130.6 km of Highway BR-174 and 1249.4 km of secondary roads in the settlement projects and their surroundings (Fig. 1). The study area, which comprises 6657.3 km^2, was delimited by clipping a Landsat 8 image for 9 June 2016 (row 231, path 60) and intersecting it with part of scenes 20NQG and 20NQF of the vector grid of the Sentinel-2 satellite (https://www.instrutorgis.com.br/download-da-grade-do-satelite-sentinel2/). The vegetation cover is composed of dense rain forest (in its vast majority), in addition to mosaics of *campinarana* (oligotrophic woody vegetation) and ecotone areas between *campinarana* and dense rain

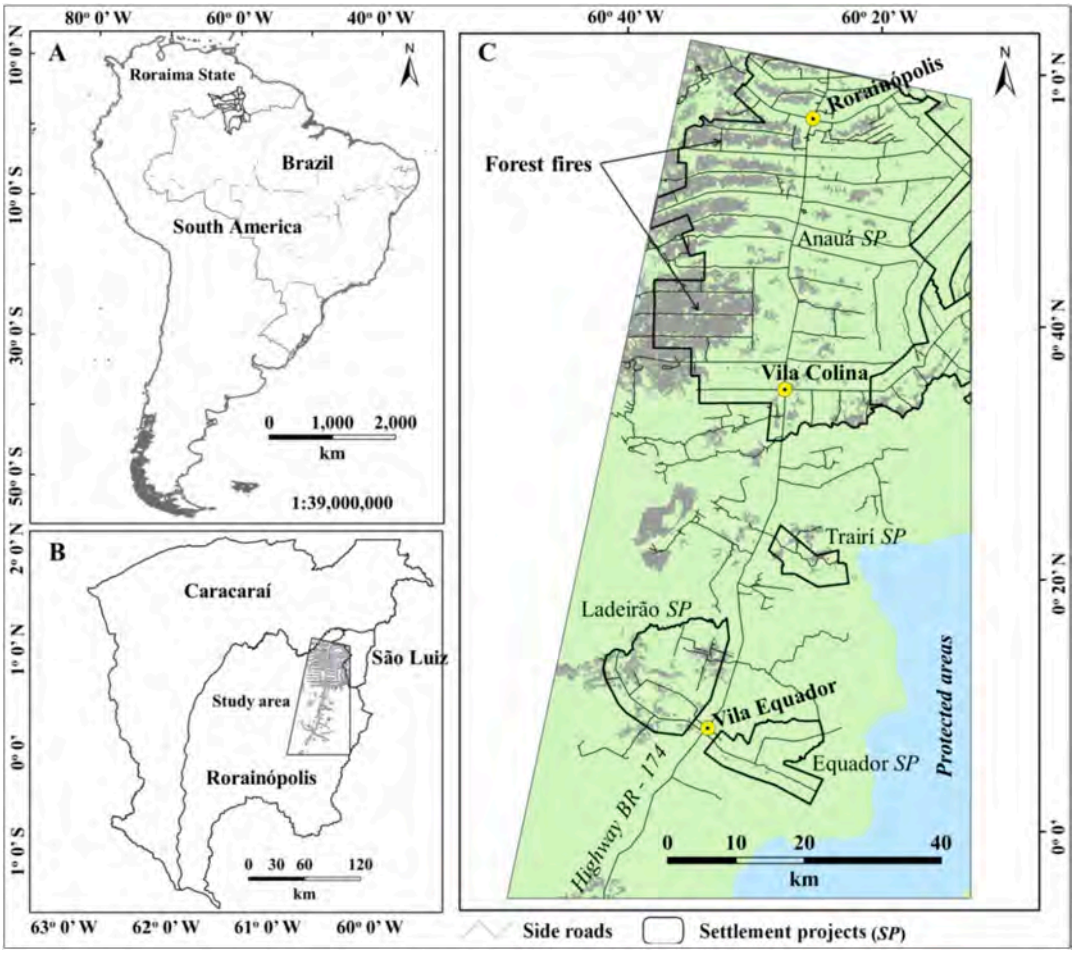

Fig. 1. (A) Map of South America showing the state of Roraima. (B) Municipalities and the location of the study area. (C) Detailed map of the study area.

forest (Barni et al., 2016). Under the Köppen classification system, the region's climate is *Af* (equatorial forest climate) (Alvares et al., 2014).

2.2. Databases

The database consisted of 1.) A vector grid from the Sentinel-2 satellite (which was used to delimit the study area), 2.) Landsat 5 and 8 images from 2007 to 2016 for path/row 231/60, obtained from the US Geological Survey (USGS, 2016) (which were used to map the dynamics of SL and fire) 3.) A Shuttle Radar Topography Mission (SRTM) image (USGS, 2016) (which served to represent the altitude and the slope in the study area), 4.) A vector map of forest types (Brazil, PROBIO, 2013), 5.) A map of deforestation and non-forest obtained from PRODES (Brazil, INPE, 2020), 6.) A vector map of forest fires (Barni et al., 2017) (used to represent the burned area), 7). A map of total forest biomass (live + dead and above + belowground) in Roraima (Barni et al., 2016) (used to estimate biomass loss and affect by fire), 8.) Vector maps of roads and rivers, 9.) A vector map of hot spots between 1 December 2015 and 23 March 2016 from the AQUA-MT reference satellite (http://queimadas.dgi.inpe.br/queimadas/bdqueimadas/) (used to represent the initial scenario of fires in the study area using the weights-of-evidence method), 10.) Forest inventory data on observed fire and tree mortality in 17 transects measuring 4 × 250 m (1.7 ha) at the locations of fires that occurred in the study area during the 2015/2016 El Niño event (Table S2) (used to estimate the biomass loss at the plot level).

For the processing of variables (maps), analyses were performed using the Quantum Gis (QGis) Desktop 2.18.15 (https://www.qgis.org/) geographical information system (GIS). Maps 2 to 9 (except map 7) and products derived from these have been used for analyzes with the weights-of-evidence method (Barni et al., 2015b, 2020; Soares-Filho et al., 2006; Leite-Filho et al., 2021) in Dinamica-EGO 5.0 software (https://csr.ufmg.br/dinamica/). Statistical analyses were performed using R version 3.6.0 software (https://www.r-project.org/).

The database included information on authorizations for logging (authorized area in ha and volume in m^3) in the area licensed for "alternative land use" (deforestation) from 2010 to 2015 (Table S3); the database also included information on "Sustainable Forest Management Plans" from 2017 to 2020 (Table S4), which were used to support the analyses. These data were provided by the State Foundation for the Environment and Water Resources (FEMARH) under the technical collaboration agreement 001/2020 between FEMARH and the State University of Roraima (UERR). The methodological sequence for obtaining and analyzing the data followed the flowchart in Fig. 2.

2.3. Methods

2.3.1. Fire severity

Assessment of the severity of the fire consuming the combustible material and killing a fraction of the living forest biomass above and below ground was conducted according to the technique recommended by Fernándes-Manso et al. (2016), using vegetation indices, including the normalized difference vegetation index (NDVI). In this approach, the NDVI values were extracted from the Landsat 8 image for 9 June 2016 (231/60) corresponding to the burned forest in the study area, and discrimination was made among four increasing levels of fire severity: light, moderate, strong and very strong (Table 1). The break points of the classification intervals for NDVI values were set automatically by the software (Jenks natural breaks: Dent, 1990; Slocum, 1999) in five classes, with the fifth class (-1 to 0.2246) corresponding to pixels with spurious values, which were excluded from the analysis. In the study by Fernándes-Manso et al. (2016), based on visual interpretation of images from the Pleiades-1A/1B sensor, the 'light' class corresponded to minor or insignificant damage from the fire scar; the 'moderate' class corresponded to a moderately damaged area; the 'strong' severity level corresponded to a highly damaged area and; the 'very strong' severity level corresponded to an area totally destroyed by fire. Although the study by

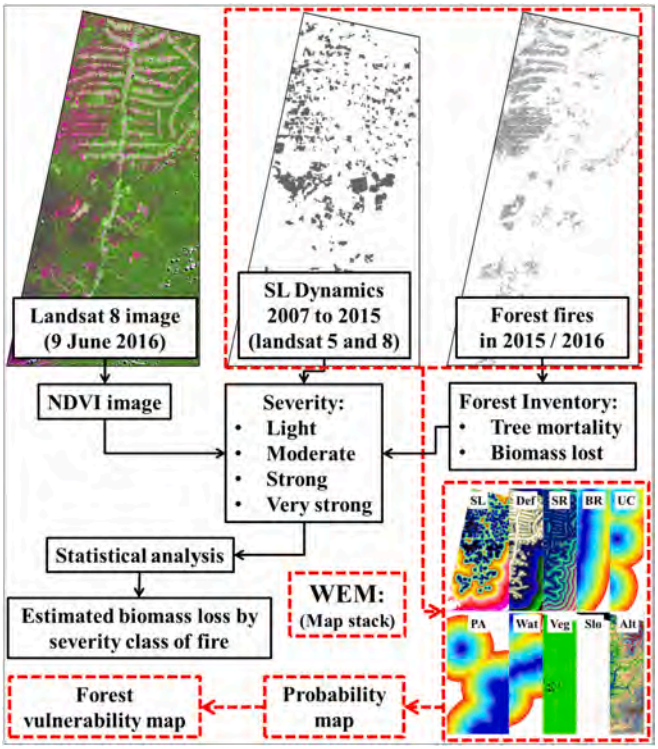

Fig. 2. Flowchart of the methodology applied in the study area to obtain and analyze the data. SL = selective logging; NDVI = normalized difference vegetation index. WEM = weights-of-evidence method. Continuous variables (distance map): SL = selective logging, Def = deforestation, SR = secondary roads, BR = BR – 174 highway, UC = urban centers, PA = protected area and Wat = water. Categorical variables: Veg = vegetation, Slo = slope and Alt = altitude.

Table 1
Increasing levels of fire severity observed in the study area.

Level	Class	NDVI (this study)	*NDVI
0	Light	0.4082 to 0.6031	0.5840 to 0.6195
1	Moderate	0.3641 to 0.4081	0.5225 to 0.5700
2	Strong	0.3140 to 0.3640	0.4095 to 0.4495
3	Very strong	0.2247 to 0.3139	0.2267 to 0.2637

* Values estimated from Fernándes-Manso et al. (2016).

Fernandes-Manso et al. (2016) was carried out in a region of Spain dominated by *Pinus pinaster* Ait and *Quercus pyrenaica* Wild, which is a type of a vegetation completely different from that in the Amazon, it is important to highlight that in our study we only used the nomenclature for fire-severity classes based on these authors, corresponding to the classes for separation of the NDVI values obtained in our study area. Our choice was based on the familiarity with the use of NDVI and the evaluation of various vegetation indexes carried out by Fernandes-Manso et al. (2016). These authors indicated that the NDVI achieved scores similar to that of the normalized burn ratio (NBR) in a Cox and Snell pseudo-R^2 test (0.430 and 0.450) and in a McFadden pseudo-R^2 test (0.289 and 0.247) for NDVI and NBR respectively. In our study, NDVI was highly correlated with NBR (Figure S1 and S2; Table S5).

2.3.2. Estimation of biomass loss by fire-severity class

We used tree mortality or biomass-loss levels (inventory data) to numerically define these classes and associate them with the corresponding severity levels. To estimate biomass loss by fire-severity class, we used loss fractions of forest biomass (Mg ha^{-1}) derived from the database for the forest inventory in the 17 transects (4 × 250 m: 1.7 ha) carried out between 11 March and 6 April 2016 for trees with DBH ≥ 10 cm. In the 17 plots (14 plots with SL and three plots without SL), 1180 individuals (694 individuals ha^{-1}) were inventoried, of which 239

individuals (20.3%) had been killed by fire. Trees that were considered to have been "killed" were observed in the field (1–3 months after the fires) and judged to be dead based on lack of leaves, appearance of the bark and signs of severe damage from the fire. The percentages for estimating biomass loss in trees with DBH ≥ 10 cm were derived from the forest-inventory data. The 10.4% loss percentage represented by the aboveground dead biomass (litter) and the 2.4% aboveground biomass loss in dead trees with DBH < 10 cm were derived from the study by Barbosa and Fearnside (1999) (Table 2).

The volume is converted to biomass using the average basic density of 0.770 of the 11 species that contributed the most wood volume to nine sawmills surveyed in 2013 in Rorainópolis by Crivelli et al. (2017), based on basic density values from Fearnside (1997), Nogueira et al. (2005) and Silveira et al. (2013), weighted by their respective percentages of the volume processed by the sawmills (Table S6). "Basic density" of wood is oven-dried mass divided by saturated volume. A calculation is made of the biomass removed in the harvested logs, together with the loss of aboveground live biomass in the crowns and stumps of the harvested trees and in collateral damage to unharvested trees caused by the logging operations (Supplementary Material, Section 1.7: Table S7). The biomass lost (35.67 Mg ha^{-1}), when divided by the average total biomass value (435.3 Mg ha^{-1}) of the dense ombrophilous forest in the study area (Barni et al., 2016), results in a loss fraction of 0.082. In this approach it is assumed that the SL had already been removed this fraction of the biomass, and the fraction is therefore applied as a constant regardless of the fire-severity class.

To derive these loss percentages and assign the biomass values corresponding to each severity class, the DBH ≥ 10 cm information on the inventoried trees (1180 individuals) was converted into aboveground dry biomass according to the model ln (P) = β0 + β1 ln (DBH) + ε, proposed by Higuchi et al. (1998), where P is the fresh weight (kg^{-1}) of the biomass, β0 (-1.497) and β1 (2.548) represent the regression parameters (intercept and slope), ln is the natural logarithm and ε is the random error. Values for fresh biomass (kg ha^{-1}) were converted to dry biomass (Mg ha^{-1}) based on the mean water content of 40% found by Higuchi et al. (1998) (Table S2).

In order to represent the fire-damage classes overlapping the inventory transects, a 15-m buffer was created around the length of each transect. Next, the fire-severity class values were extracted from a raster file intersecting the buffer areas (Fig. 3A); the average percentages were attributed for the biomass loss corresponding to each class indicated in the pixels, which were estimated by the model, and the total biomass was calculated for the 17 transects (Fig. 3B).

2.3.3. Biomass of fire-affected areas by forest type

The biomass (Mg ha^{-1}) affected by the fires in each vegetation type was calculated using the biomass map prepared by Barni et al. (2016) in a grid-cell (raster) format. This biomass estimate was based on bole volumes of individual trees ≥ 31.8 cm DBH surveyed by the RADAMBRASIL project (Brazil, RADAMBRASIL, 1973-1983) in 298 1-ha plots (of which 119 were in Roraima and the remainder within 100 km of the state's borders). Volumes were converted dry biomass based on the wood basic density by species from Fearnside (1997), and adjustments for crowns, small trees, hollow trees, irregular trunks and other components were based on Nogueira et al. (2008).

Initially the biomass map was intersected with the forest-typology map, also in raster format, and the study area was cut out. The study area contained three vegetation types: Dense ombrophilous forest (DS), *Campinarana* (Ld) and Ecotones (LO). Note: the two-letter vegetation codes are those used by the Brazilian Institute for Geography and Statistics (IBGE). The biomass map for the study area was intersected with the forest-fire raster map (value = 1). These map-algebra operations were performed using the raster calculator in the GIS:

$$\sum \text{Biomass}_i = \left(\sum \text{pixels}_i * BM_i * PA * F_i\right) \Big/ 10,000$$

Where: $\Sigma Biomass_i$ is class i biomass (Mg); $\Sigma pixels_i$ are pixels of type / class i; BM_i is the biomass map (Mg ha^{-1}) of type / class i; PA is the pixel area and F_i is the fraction of severity class i. The same procedure (minus F_i) was carried out to calculate the biomass loss caused by deforestation up to 2016 in the study area (Brazil, INPE, 2020).

Table 2
Fractions of biomass loss from fire used in the GIS raster calculator for calculations of biomass loss by fire severity class.

Severity	Litter	DBH < 10 cm	DBH ≥ 10 cm	Loss fraction
Light	0.104	0.024	0.022	0.150
Moderate	0.104	0.024	0.074	0.202
Strong	0.104	0.024	0.151	0.279
Very strong	0.104	0.024	0.329	0.457

2.3.4. Characterization of selective logging in the study area

To characterize SL in terms of the area that was logged and affected by understory forest fires in the entire study area, a systematic mapping of timber activity in the region was carried out between 2007 and 2015 using 16 satellite images (path/row 231/59 and 231/60) from Landsat 5 (2007 to 2011) and Landsat 8 (from 2013 to 2015) (Table S8 and Figure S3). For this purpose, RGB and NDVI images were interpreted visually, proceeding to manual editing in vector files of the SL areas in each image, as in Barni et al. (2015a) (Supplementary material: Section 1.8). As a way of assessing the influence of SL on the spread of fire and on the severity classes in the study area, tests were carried out to compare the NDVI values from 2016 with the NDVI values of the images from 2010, 2013, 2014 and 2015 at the same geographical coordinates in areas affected by fires and with a history of SL. Additionally, analyses of severity of fire were carried out according to the year of selective logging occurrence (Table S9).

2.3.5. Fire-vulnerability map with weights-of-evidence method

The map of the forest's vulnerability to fire was obtained from the calculation of the transition-probability map using the weights-of-evidence method (Supplementary material: Figures S4, S5 and S6). This method stores information as numerical values that are spatially referenced (x and y coordinates) representing the contribution (evidence) of each variable in favoring or inhibiting the occurrence of the event under study (in our case, fire), based on the occurrence of this event in the past. In other words, the weights-of-evidence method has the ability to capture the influence of a set of variables related to the spatial occurrence of a given event in the past and use that evidence (weights-of-evidence coefficients) to build a spatial-probability map for the occurrence of the event in question. This ability has often been exploited in simulating future deforestation and forest-fire scenarios in the Amazon (Barni et al., 2015b, 2020; Leite-Filho et al., 2021; Silvestrini et al., 2011; Soares-Filho et al., 2006).

For the preparation of the vulnerability map of the forest to understory forest fires, a methodological sequence was used that involved the preparation of initial and final scenario maps in Dinamica-EGO software. First, a land-use map was prepared with the value classes (1) Deforested, (2) Forest and (3) Fire. The latter consists of 216 hot spots detected in the study area by the AQUA-MT satellite between 1 December 2015 and 23 March 2016 (the time window when fire occurrences intensified in the study area), transformed into pixels, representing the fire class (value = 3) before the spread of the fire (initial scenario). Second, a land-use map was prepared with the same classes, but with the fire class applied to all of the fire spread detected in the study area in 2016 (final scenario), which was obtained from the mapping carried out by Barni et al. (2017) (Fig. 4).

Twelve maps were created with the same number of columns and rows. Seven of the maps were for environmental variables: (1) forest (vegetation), (2) deforestation, (3) fire, (4) SL, (5) SL class year (area of polygons of SL mapped each year), (6) hydrography (water courses), (7) relief and (8) slope. Four maps were for infrastructure: (9) urban centers,

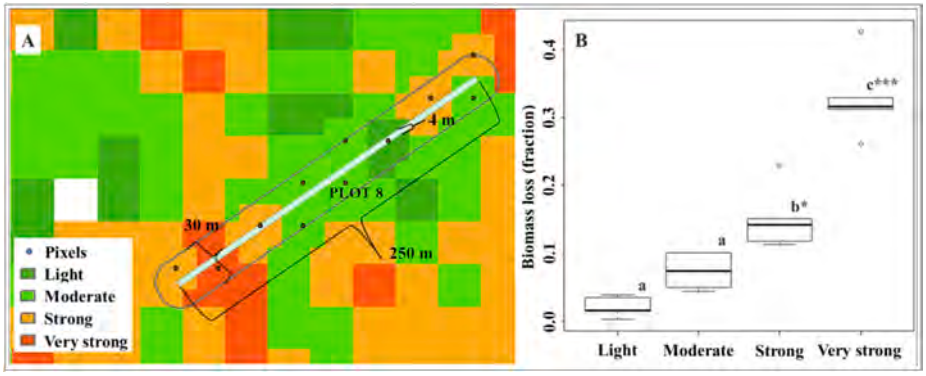

Fig. 3. (A) Levels of fire severity along a plot inventoried in the field and (B) corresponding rates (fractions) of biomass loss. Equal letters = not significant; * = significant at 5%; *** = significant at 0.1% statistical probability.

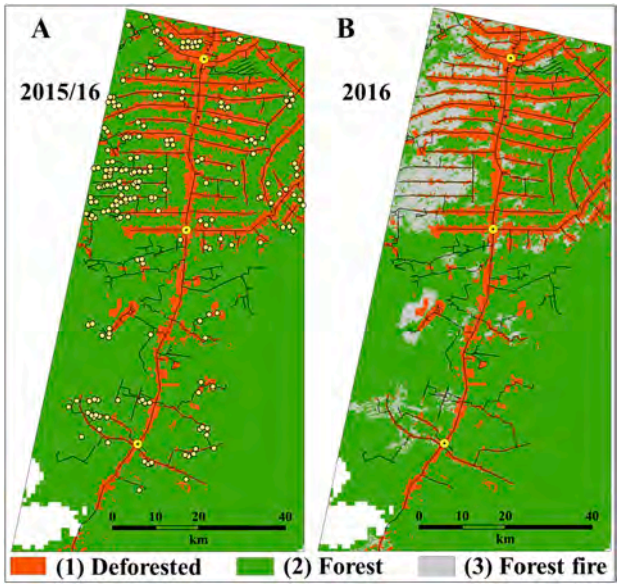

Fig. 4. Input scenarios for the method of calculating the weights-of-evidence using Dinamica-EGO software. (A) 2015–2016 Scenario (initial map) prepared with hot spots between 1 December 2015 and 23 March 2016. (B) Scenario in 2016 (final map) after the occurrence of fires in the region.

(10) secondary roads, (11) BR-174 and (12) protected areas (Indigenous Lands + conservation units). This step also involves the creation of maps of distance-intervals (ranges) to fire scars for eight continuous variables and creation of class intervals for the other four variables (vegetation, altitude, slope and SL class year), which are considered to be categorical. The mapped variables (as a data stack) served as inputs for calculating the weights-of-evidence coefficients (Figures S3 and S4) using Dinamica-EGO software.

In addition to these initial procedures, a transition matrix was also calculated, which is an array of the rates that the software uses to perform the transitions of pixels between states. For example, a pixel representing forest (value = 2) at time t_1 can convert to a pixel representing fire (value = 3) at time t_2, in a simulated scenario. In the simulation model, the transition matrix provides the number of pixels that are ready for the change of state, while the transition probability map directs the change to the areas of greatest probability.

Correlation tests were performed to determine the association between variables and to assess their spatial dependence (Bonham-Carter, 1994). Correlations with a value of $r \geq 0.5$ were considered to represent a strong association between the variables (Cohen, 1988). These steps were performed using Dinamica-EGO software (Supplementary Material).

2.3.5.1. Assessment of the effect of SL on fire spread. It is important to note that fire-severity classes were not considered in assessing the effect of SL on the spread of fire in the forest. To assess fire spread we considered five vulnerability classes that were calculated and mapped using the weights-of-evidence method. The following procedures were performed to test the effect of SL on the spread of fire in the study area: 1.) making a transition-probability map using all of the variables in the database; 2.) making a transition-probability map using all of the database variables except for the SL variable; 3.) making a transition-probability map using only database variables with little or no correlation with SL and SL class year and; 4.) making a transition-probability map using only SL and SL class year together with the database variables with little or no correlation with SL. These procedures were also carried out for the variables "deforestation" and "secondary roads," which were highly correlated with SL in the study area (Table S10). The sizes (km^2) of five classes of vulnerability of the forest to fire were then compared on the maps. The difference (in %) in the size of the area of the class with the greatest vulnerability to fire was calculated by comparing the map made using the set of variables that included both SL and the variables without correlation with SL with the probability map calculated only with the set of variables without correlation with SL. The percentage difference was considered to represent the effect of SL on the spread of fire in the study area. For the purpose of comparison and to serve as a reference in order to support the discussions, the same procedure described above was performed for the variables "deforestation" and "secondary roads." The effects of the variables were also expressed in terms of biomass (Mg) vulnerable to fire in the study area. In this case, only the area in the class with the highest probability of fire was considered for the purpose of applying the biomass calculations in making the comparison between the models.

2.3.6. Validation of models

To validate the simulation models, the reciprocal-similarity comparison technique was used (Soares-Filho et al., 2008) based on adaptation of the fuzzy-similarity method and the Kfuzzy method, which is considered to be equivalent to the Kappa statistic and takes into account the fuzziness of both location and category within a cell neighborhood (Hagen, 2003). The method is based on the state of the central cell of each window, observing the similar and divergent states of the cells in its neighborhood (or proximity) as a parameter of comparison between the maps. In this approach, the simulated fire scenario is compared with the 2015–2016 scenario (initial scenario) and with the 2016 scenario (map of fire that actually occurred) using "windows" of different sizes in an exponential decay function (truncated outside of a window size of 11 × 11 cells) (Figure S7). The exponential decay function records the scores of the comparisons between maps produced with increasing window sizes (3 × 3 pixels, 5 × 5 pixels, …, 11 × 11 pixels), and the test result (%) is returned as a .csv table file (Figure S7). The window acts as a filter covering all of the lines in the raster map to make the comparison

(Figure S7). Models are generally considered to be valid for simulation when the similarity value for the maps being compared is ≥ 50% (Barni et al., 2015b, 2020). The tests were carried out in a sub-model of the Dinamica-EGO software (Figure S8).

3. Results

3.1. Areas of occurrence

The area of understory forest fires that occurred in our study area during the 2015–2016 El Niño event totaled 682.2 km^2, affecting 12.6% of the remaining original forest. The cumulative deforestation in 2016 (observed since the 1970s and 1980s) in this region (1102.1 km^2) represented 16.6% of the study area and 16.9% of the area that was originally forest (Table S11). The cumulative deforestation attributed to the portion of the municipality of Rorainópolis located within the study area represented 90.8% of the deforestation observed in the entire municipality up to 2016 (1151.2 km^2: Brazil, INPE, 2020) (Table S1).

In the study area, SL mapped between 2007 and 2015 totaled 644.8 km^2. Of this SL area, 28.0% (180.7 km^2) was also affected by understory forest fire (Table S11 and Figure S3).

3.2. Estimation of biomass in areas affected by forest fires

The largest amount of biomass affected by the fires (22.7 × 10^6 Mg) was under ombrophilous forest (dense rain forest) and the smallest (0.3 × 10^6 Mg) was found in ecotone forests (Table S12). The fire scars spread along the BR-174 and its secondary roads from the vicinity of the Rorainópolis municipal seat to an area near Vila Equador (Fig. 1).

The total biomass affected by fires in our study area was estimated at 26.2 × 10^6 Mg, while the biomass affected by fires in the SL area was estimated at 6.7 × 10^6 Mg (Table S12). This represents 24.1% of the total biomass in areas subjected to SL, estimated at 27.9 × 10^6 Mg. Estimation of forest biomass was performed for each forest type, separating areas of SL and areas without SL are presented in Table S13. Estimates of biomass loss from deforestation until 2016 are presented in Table S14 for in the study area as a whole and separately for each forest type.

3.3. Fire-severity gradient area

The most widespread severity level in the study area was the light-intensity class (39.1%), considering areas burned without SL. When considering the same severity level but in areas with SL, the light-intensity class decreased by 27.9% in relation to the area without SL. On the other hand, when considering the highest level of fire severity (very strong) the area under SL shows an increase of 85.9% in terms of incident area of this class in relation to the area without SL (Table 3). This means that, if a hectare of forest burns, it is 85.9% more likely to be a very-strong burn if that hectare had been previously logged.

3.4. Vulnerability of the forest to understory fires in SL areas

The assessment of the vulnerability maps showed that SL influenced the spread of fire in the study area during the 2015/2016 El Niño event within the fire-severity classes. Analyses of NDVI images show a positive correlation between fires and the logging carried out in years immediately prior to the fires. On the other hand, this effect was not observed when comparing the NDVI values of the images of locations that had been subjected to SL in 2010 with the NDVI values obtained in the same places after the 2015/2016 fires (Figure S9).

These results are confirmed by annual SL data from satellite images (Table S8) and analysis of the distances from the edge of the forest to the locations of the fires and the SL. The largest fire recorded in areas affected by SL (161.2 km^2) occurred in the distance range from 0 to 1200 m, representing 89.3% of the total spread of fire (180.5 km^2) in the area with SL. The years that contributed most to the area of SL were 2013, 2014 and 2015, providing the SL-disturbed area through which the fires crossed and spread to neighboring areas (Fig. 5A). Beginning in 2011 there is a strong inversion of the severity classes, with locations with more-recent SL burning with greater severity in the 2015/2016 fires (Fig. 5B, Table S9).

3.5. Estimation of biomass loss by fire-severity class

The biomass affected by forest fires totaled 26.4 × 10^6 Mg (Table 4), with the biomass in the fire-affected SL areas totaling 6.7 × 10^6 Mg (25.4 of the fire-affected biomass), while the biomass computed outside of the SL areas represented 74.6%. The highest severity level ("very strong") affected, proportionally, 84.6% (14.4% versus 7.8%) more biomass in SL areas than outside of these areas (Table 4).

The largest amount of biomass killed by fires (1.8 × 10^6 Mg; mean 79.1 Mg ha^{-1}) was in the "moderate-loss" class, representing 30.8% of the total estimated biomass. The smallest amount of biomass (1.1 × 10^6 Mg; mean 176.3 Mg ha^{-1}) was in the class with the highest fire severity, representing 19.5% of the total biomass killed by the fires. Considering the level of greatest severity, the loss in the SL areas was, proportionally, 68.3% greater than in the areas without SL (27.6% versus 16.4%, respectively) (Table 5).

An increase in biomass loss with increasing fire severity is apparent, and the loss is greater at each intensity of fire if the area had been subjected to SL. If one considers only omprophilous forest, which represents 78.1% of the area affected by fire and 87.8% of the logged area, the differences between logged versus unlogged areas are significant Kruskal-Wallis test, $p < 0.05$) (Fig. 6). If all forest types are considered, the data suggest the same pattern but the added variation from forest-type effects makes the difference statistically nonsignificant (Figure S13).

3.6. Calculation of the weights-of-evidence coefficients

Of the 12 variables used to calculate the coefficients of the WEs, six showed a strong correlation between them ($r \geq 0.5$). The highest correlation was between cumulative deforestation in the study area and secondary roads, with $r = 0.86$, and the second-highest value was between SL areas with secondary roads, with $r = 0.78$ (Table S10). Theoretically, this means that these variables are overlapping in the model and would explain, basically, the same things. When two variables are correlated, it is recommended that one of them be removed from the prediction model, with the variable that remains being the one

Table 3
Area of severity classes of understory fire without selective logging and with.

Severity	Total		Wo/SL		W/SL		Difference with SL%
	Area (km^2)	%	Area (km^2)	%	Area (km^2)	%	
Light	246.5	36.2	195.5	39.1	51.0	28.2	−27.9
Moderate	229.0	33.5	170.6	34.0	58.3	32.3	−5.3
Strong	140.7	20.7	95.5	19.1	45.2	25.0	31.2
Very strong	64.9	9.6	38.8	7.8	26.1	14.5	85.9
Total	**681.1**	**100**	**500.4**	**73.5**	**180.7**	**26.5**	-

W/SL = with selective logging. Wo/SL = without selective logging.

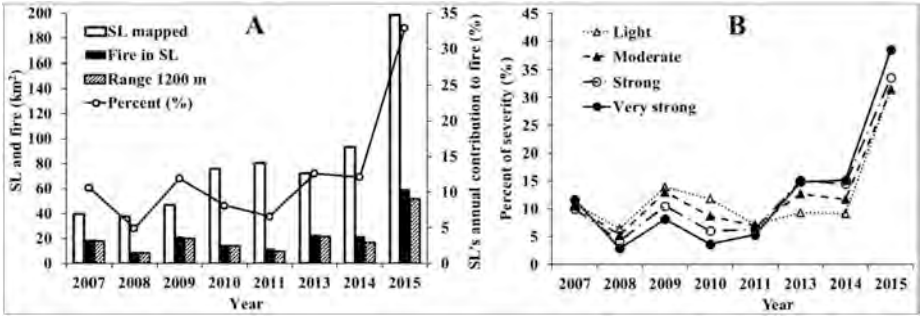

Fig. 5. (A) Annual contribution of areas impacted by SL that were burned during the 2015/2016 El Niño event in the study area. (B) Gradient of fire severity depending on the year of logging.

Table 4
Estimated biomass affected by fire for each fire-severity class considering all forest types.

Severity	Area (km^2)	Wo/SL (10^6 Mg)	% of biomass	Area (km^2)	W/SL (10^6 Mg)	% of biomass	SL (10^6 Mg)	% of biomass	Total (10^6 Mg)	%
Light	195.5	7.5	38.1	51.1	1.9	28.2	0.17	28.3	9.4	35.6
Moderate	170.6	6.8	34.6	58.3	2.2	32.3	0.19	32.4	9.0	34.0
Strong	95.5	3.9	19.5	45.2	1.7	25.2	0.15	25.2	5.6	21.2
Very strong	38.8	1.5	7.8	26.1	1.0	14.4	0.09	14.4	2.5	9.3
Total	500.4	19.8	100.0	180.7	6.7	100.0	0.6	100.0	26.4	100.0

W/SL = with selective logging. Wo/SL = without selective logging.

Table 5
Estimation of biomass killed by fire for each fire-severity class considering all forest types.

Severity	**Wo/SL**			**W/SL**			**Total**		
	Biomass (10^6 Mg)	**%**	**Mean (Mg ha^{-1})**	**Biomass (10^6 Mg)**	**%**	**Mean (Mg ha^{-1})**	**Biomass (10^6 Mg)**	**%**	**Mean (Mg ha^{-1})**
Light	1.1	26.5	58.1	0.3	17.8	55.7	1.4	24.2	57.6
Moderate	1.4	32.0	80.3	0.4	27.5	75.5	1.8	30.8	79.1
Strong	1.1	25.0	111.8	0.5	29.5	104.6	1.5	26.2	109.5
Very strong	0.7	16.4	181.1	0.4	27.6	169.3	1.1	19.5	176.3
Dead	**4.3**	**21.7**	**84.1**	**1.6**	**23.9**	**92.6**	**5.9**	**22.3**	**86.4**
Affected	**19.7**	**7.9**	-	**6.7**	**24.3**	-	**26.4**	**9.5**	**387.6**
Total	**249.8**	**90.1**	-	**27.6**	**9.9**	-	**277.4**	**100.0**	-

W/SL = with selective logging. Wo/SL = without selective logging.

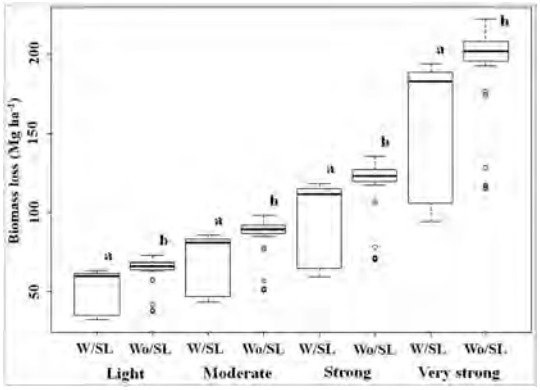

Fig. 6. Biomass loss (Mg ha^{-1}) by fire-severity class in areas with SL (W/SL) and areas without SL (Wo/SL) considering only ombrophilous forest. The different lower-case letters above the boxes indicate that there was significant difference ($p < 0.05$) between the loss of biomass by fire in previously logged areas and unlogged areas within each severity class.

that is more consistent with the conceptual or theoretical model of the phenomenon to be modeled or predicted (Soares-Filho et al., 2008).

The SL variable (a continuous variable) had the highest value for the weights-of-evidence coefficient (W = +1.15 to 0.99) between 0 and 480 m away from the fires, and this coefficient decreased to a value close to zero at ~ 2000 m. Similar behavior was also observed for the variables "secondary roads" (W = + 0.68 to 0.83) and "deforestation" (W = + 0.44 to 1.06) in the first 480 m from the areas affected by fires (Fig. 7). These distances were expressed as intervals of 120 m in the Dinamica-EGO software and are compatible with the 30-m pixel size of the Landsat 8 image and of the weights-of-evidence maps of the variables used in the study. The response or dependent variable "fire" had the highest weights-of-evidence coefficients. These values indicate a high probability of transition from forest pixels (value = 2) located close to the edges of the forest (value = 1) to pixels representing burned areas (value = 3) on the simulated or modeled map. Note that most of the variables strongly repel the transition of pixels located from ~ 2500 to 5000 m, with the weights-of-evidence coefficients having values less than zero.

The behavior of the weights-of-evidence coefficients of SL (and of other variables correlated with SL) shown in Fig. 7 can be explained by the heavy fragmentation of the forest in the study area. For example, on both sides of Highway BR-174 there are secondary roads and cumulative deforestation adjacent to these roads (both inside and outside of settlement projects). The roads fragment the forest at regular intervals of 2 to 4 km, depending on the degree of deforestation at each site. The sizes of the forest fragments limited the weights-of-evidence (W^+) of the main variables that explain the behavior of fire in the study area at distances between 1000 and 2000 m from the edge of the fire scars in the forest (Fig. 7).

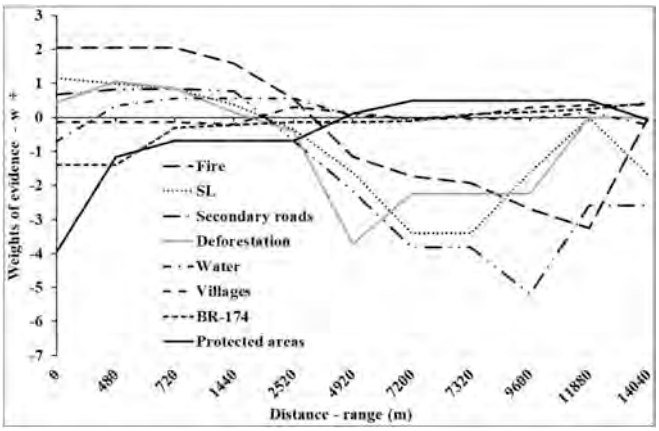

Fig. 7. Coefficient of the weights-of-evidence (W^+ or W^-) for seven variables that explain the occurrence of forest fires (dependent variable) in the study area. The distance is subdivided into multiple intervals of 120 m.

Corroborating these results, the areas affected by forest fires and SL gradually decreased in successive 120-m intervals from the edge of the forest up to a distance of 1200 m. The first interval (0 to 120 m) had the largest area affected by fire (114.9 km^2; 20.1%) and also had the largest area affected by SL (113.8 km^2; 24.3%). Considering the entire range of 1200 m from the edge of the forest, the area burned totaled 571.7 km^2 (83.9% of the 682.2 km^2), SL areas totaled 468.8 km^2 (72.7% of the 644.8 km^2) and the SL areas in areas affected by fire totaled 161.2 km^2, or 89.4% of the 180.4 km^2 total (irrespective of distance: Table S15) burned in the SL areas (Fig. 8A; Table S15). The ratio of the area affected by SL to the area affected by fire (SL/Fire) showed a continuous growth beginning with the second distance interval (121–240 m from the forest edge) up to a distance of 1200 m (Fig. 8B). The SL area affected by fire as a percentage of the SL area as a whole (SL × Fire/SL) had behavior opposite to that of SL/Fire; that is, the areas of occurrence decreased with increasing distance from the edge of the forest. In turn, the area of SL affected by fire as a percentage of the area burned as a whole (SL × Fire/Fire) showed a more stable behavior when compared to the other variables, with 20.6% in the first interval, increasing to 26.5% in the second interval, and stabilizing at 31.1% (on average) from the third to the last interval (241–1200 m).

These results indicate a strong influence of SL on the spread of the fire in the study area, especially as exemplified by SL/Fire and SL × Fire/Fire (Fig. 8B). Although this analysis includes only the variable SL, all other variables were also exposed to the same environmental context in the study area. The values of the weights-of-evidence calculated for each distance range of the variables contained in the models ensure the statistical independence of the results (Bonham-Carter, 1994).

3.7. Model-validation results

The models were validated in windows that ranged in size from one pixel (30 m) to seven pixels (210 m). The greatest similarity (65.9%) between the models and considering all windows was observed in the model containing all variables. This map reaching 50% similarity in a ~ 65-m window. On the other hand, the worst performance was by the map from the model that used only the variables that were not correlated, reaching 50% similarity in a ~ 108-m window. The other three models had approximately the same performance, with results between the two extremes and reaching 50% similarity in a window of ~ 80-m (Figure S10).

3.8. Vulnerability of the forest to understory fires by probability range

Considering ranges of vulnerability to the occurrence of forest fires in the probability map, areas vulnerable to fire increased by 266.2% in the range with the highest vulnerability when SL and SL class year were present, as compared to the reference model (Figure S11). Likewise, when the probability map was modeled with the presence of secondary roads, the area of greatest vulnerability to fire increased by 360.4% compared to the reference model (Fig. 9; Table S16).

All of the vulnerability maps had the class with the lowest probability of fire (0.0004 to 0.1488) as the most representative area in the modeling. This can be explained simply by the fact that these areas are relatively far from the sources of ignition by human action and, therefore, would be naturally protected. This can be clearly seen in continuous blocks of forest on both sides of Highway BR-174 in the map calculated with the entire set of variables (areas south of Vila Colina in the south-central part of the map) (Fig. 10A). To a lesser extent it can also be seen in Fig. 10C. On the other hand, the map considered as a

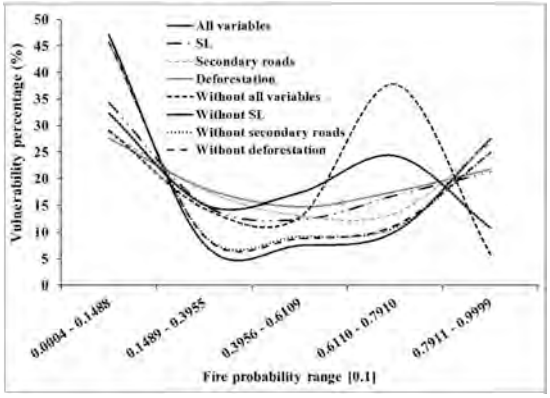

Fig. 9. Percentage of vulnerability of the forest as a function of the ranges of probability (0.1) of fire occurrence in the study area.

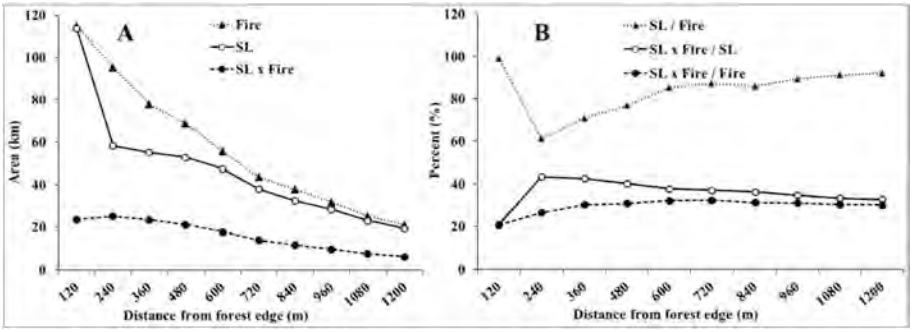

Fig. 8. Fire and SL behavior as functions of distance from the forest edge (in 120-m intervals). (**A**) Areas (km^2). (**B**) Interaction between fire and SL (%). Fire = Area affected by fire; SL = Area of SL; SL × Fire = Area of SL affected by fire; SL/Fire = Ratio of the area affected by SL to the area affected by fire; SL × Fire/SL = The SL area affected by fire as a percentage of the SL area as a whole; SL × Fire/Fire = Area of SL affected by fire as a percentage of the area burned as a whole.

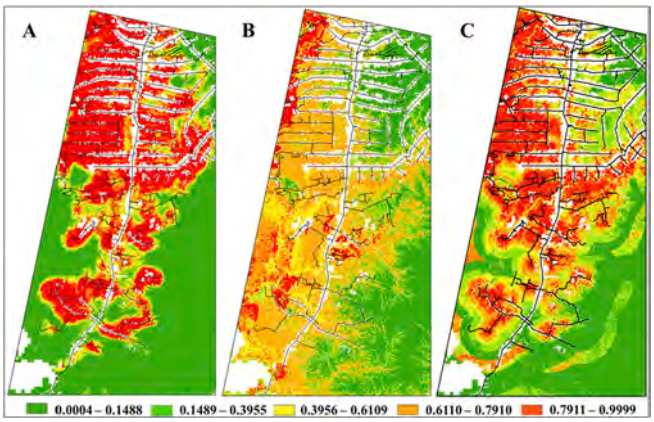

Fig. 10. Maps of vulnerability of the forest to understory fire. In (A) forest vulnerability map calculated with the entire set of variables (n = 12). In (B) vulnerability map calculated from a set of three variables (altitude, vegetation and slope) that are not correlated with SL (reference model). In (C) forest vulnerability map calculated from the variables not correlated with SL and plus the SL and SL class year variables. The legend below the figure shows the ranges of probability [0.1] of the forest being affected by fires.

reference, which represented fires calculated by the model composed of three explanatory variables not correlated with the SL (altitude, slope, and vegetation) (Fig. 10B), showed these blocks of forest as vulnerable to fire. This effect can be explained by the absence of protected areas in the model's data set. Because the protected areas were correlated with SL, this effect was less evident in the calculated map containing SL in the data set. The maps of vulnerability to fires calculated with the variables "secondary roads" and "deforestation" are shown in Figure S12.

The exposure of forest biomass to fires in the study area was 457.2% higher when considering the variable "cumulative deforestation" compared to the reference model (Fig. 10B), while SL and SL class year exposed 407.0 % more forest biomass when compared to the reference model. This percentage (400.7 %) can be considered to represent the effect of SL on the spread of fire in the study area. The variable "secondary roads" exposed 591.2% more biomass to fire than the reference model (Fig. 11). Likewise, SL and SL class year exposed 266.2% more forest area to the range with the highest risk of vulnerability compared to the reference map, while deforestation exposed 9.0% more area than SL. Back roads exposed 360.4% more forest area than the reference map (Figure S11).

3.9. Effect of logging on biomass losses due to fire

The biomass losses in burned areas are summarized in Table 6, indicating a total loss of 5.22×10^6 Mg of biomass stock due to fire. In the burned areas the percentage of biomass lost is 23.2% in areas that had been selectively logged, and 21.6 % in areas without selective logging.

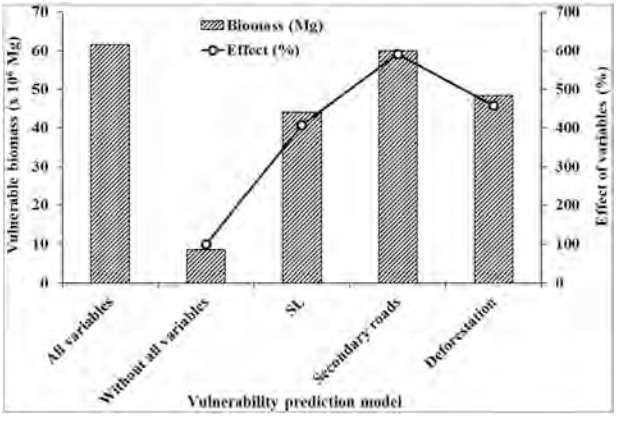

Fig. 11. Biomass vulnerable to understory forest fires in the study area.

The effects of selective logging on losses to fire are calculated in Table 7. The effect of logging in increasing the area burned resulted in 1.22×10^6 Mg of biomass loss due to fire (Column G), while the effect of selective logging in increasing the severity of fire and resulting per-hectare biomass loss in the area that would have burned anyway even without logging represents 1.25×10^6 Mg of biomass loss (Column M). As compared to the biomass loss from the logging itself (including collateral damage) of 1.69×10^6 Mg of biomass, the effect of logging on increasing the area burned increases impact by 72.5% (Column AB), and the increased fire severity increases the total fire impact to 146.5% (Column AD), that is, more than doubling the impact of the logging itself.

4. Discussion

4.1. Role of selective logging in increasing fire severity

In our study, the use of severity classes based on NDVI offered excellent insights into the severity of SL practiced in the studied area. Our approach can be considered to be a methodological advance because it can be easily used in calculating GHG emissions to the atmosphere using land-use models, reducing uncertainties, for example at the scale of Landsat pixels. Although it is a simplification for calculations of biomass loss, the use of constant values in our study (Table 2) can be justified by the difficulty (logistics and trained professionals) of obtaining the true parameters for the forest affected by the fires. This explains, in part, why the Brazilian inventories of greenhouse-gas emissions do not yet consider emissions from forest degradation by understory forest fires and selective logging (e.g., Brazil, MCTI, 2020).

The highest occurrences of burned areas and SL in the first distance intervals from the edge are characteristic of the intense fragmentation of the forest caused by human occupation in the study area. This fragmentation increases the contact between the sources of fire ignition (burning of forest biomass from deforestation and in the management of pastures and agricultural fields) and the edge of the forest (Alencar et al., 2006, 2015; Aragão and Shimabukuro, 2010).

Estimates of the biomass in areas affected by logging must be adjusted for the amounts of biomass removed by the logging. Logging slash and additional trees killed in the logging operations will remain in the forest as dead biomass (necromass) and the carbon in these components will eventually be emitted to the atmosphere either through burning or decay. An idea of the harvest intensity of the selective logging in the area can be derived from the officially reported volumes processed by sawmills in the municipality: a total of 455,347 m^3 over the 2007–2015 period (Brazil, IBGE, 2021). Although the part of our study area in Rorainópolis (Table S1) represents only 19.1% of the area of the municipality (33,579.7 km^2), it represents virtually all of the accessible area of forest outside of protected areas. The concentration of logging pressure in a relatively small space in the municipality may have induced the loggers to exploit these forest resources at high intensity, exposing the forest to greater fire hazard. On the other hand, the concentration of logging in a small area protected the currently inaccessible areas from increased fire risk.

4.2. Logging intensities in SL

Logging in the southern portion of the state is practiced in a manner similar to that practiced in other parts of the Brazilian Amazon (Nepstad et al., 1999). Like other areas in the Amazon, logging in our study area is characterized by exploitation of only a few commercial species, a low yield of sawn wood, deficiency in the application of forest management and widespread illegality in removal of wood from the forest (G1, 2018b; Gimenez et al., 2015; Lentini et al., 2005; Monteiro et al., 2010; Pereira et al., 2010).

The estimate of logging intensity that is needed in order to calculate

Table 6
Summary of biomass losses in burned areas.

	Original forest (unlogged and unburned)			SL loss			Affected by fire		Loss to fire		Percent affected biomass
	Area	Biomass stock	Biomass per hectare	Percent of original biomass	Biomass stock	Biomass per hectare	Biomass stock	Biomass per hectare	Biomass stock	Biomass per hectare	
	(km^2)	(10^6 Mg)	(Mg ha^{-1})	(%)	(10^6 Mg)	(Mg ha^{-1})	(10^6 Mg)	(Mg ha^{-1})	(10^6 Mg)	(Mg ha^{-1})	(%)
Burned areas with SL in ombrophilous forest	152.3	6.63	435.1	8.2	0.54	35.7	6.08	399.4	1.48	97.2	24.3
Burned areas without SL in ombrophilous forest	380.3	16.60	436.5	0	0	0	16.60	436.5	3.58	94.2	21.6
Total in ombrophilous forest	532.6	23.23	436.1	2.3	0.54	35.7	22.68	425.9	5.06	95.1	22.3
Burned areas with SL in *campinarana*	28.3	0.71	250.7	8.2	0.06	20.6	0.65	230.1	0.16	56.0	24.3
Burned areas without SL in *campinarana*	111.7	2.87	256.8	0	0	0	2.87	256.8	0.63	56.1	21.8
Total in *campinarana*	140.0	3.58	255.6	1.6	0.06	20.6	3.52	251.4	0.78	56.1	22.3
Burned areas with SL in ecotone forest	1.2	0.04	333.3	8.2	0.0033	27.3	0.04	306.0	0.07	86.3	28.2
Burned areas without SL in ecotone forest	8.1	0.30	370.4	0	0	0	0.26	321.0	0.06	69.8	21.6
Total in ecotone forest	9.3	0.30	323.3	0	0	0	0.30	319.8	0.13	70.1	22.1
Burned areas with SL in all forest types	180.6	7.34	406.2	8.2	0.60	33.3	6.73	372.9	1.64	90.8	24.3
Burned areas without SL in all forest types	501.3	19.77	394.4	0	0	0	19.47	388.4	4.21	84.0	21.6
Total in all forest types	681.9	27.10	397.5	2.2	0.60	33.3	26.20	384.3	5.85	85.8	22.3

the biomass present in the logged areas at the time of the 2015–2016 fires requires deduction based on the volume of logs removed and the area we mapped as affected by SL (see Supplementary Material, Section 1.7). Officially, from 2010 to 2015, 350,147.0 m^3 of logs were harvested in the municipality of Rorainópolis (Brazil, IBGE, 2021). If we consider that all of this volume of wood was obtained exclusively from our study area, where the areas authorized for deforestation totaled 124.8 km^2 in the period from 2010 to 2015, the average volume removed would be 28.1 m^3 ha^{-1}. Although this value is 44.8% higher than the value used in our calculations, in terms of volume (19.4 m^3 ha^{-1}), to deduce biomass removed by SL (35.67 Mg ha^{-1}; Supplementary material: Section 1.8) in areas that were burned and had signs of SL, the generated volume reaches 1,009,770 m^3 in 520.5 km^2 of SL polygons (19.4 × 520.5 × 100) mapped in our study area from 2010 to 2015 (Table S8). This value indicates that there may have been a logging 2.9 times (188.4%) greater than the value officially reported by the loggers (Brazil, IBGE, 2021).

Authorized forest-management projects provide another basis for comparison. Although FEMARH did not provide data on authorized forest-management plans for our study area before 2016, if we assume that in the period from 2010 to 2015 the same area was authorized annually for management as occurred between 2016 and 2019 (1,566.6 ha $year^{-1}$) (i.e., before the substantial increase in authorization in 2020), and we apply the average authorized harvest of 24 m^3 ha^{-1}, this implies an annual authorized harvest of 37,597.2 m^3 (Table S4). The total volume from deforestation authorizations in the 2010–2015 period (611,674.9 m^3; Table S3), plus the assumed forest-management authorizations (225,583.2 m^3) total 837,758.1 m^3, or 2.4 times the 350,147 m^3 officially reported as harvested in the municipality in the same period (Brazil, IBGE, 2021). This probably means that the officially reported volume is greatly understated.

Considering the 520.5 km^2 of SL area mapped between 2010 and 2015 (Table S8) and, using the same average harvest of 24 m^3 ha^{-1}, the total exploited volume would be 1,249,200.0 m^3, or ~ 3.6 times higher than that reported by Brazil, IBGE (2021) for the same time interval. Another important factor to be considered is that only 26.2% (3,114.1 ha) of the area authorized for "alternative land use" between 2010 and 2015 (12,480.9 ha) was effectively deforested by 2020. These facts hide a serious problem for the timber sector in southern Roraima and explains, in part, why many lumber companies were closed and stopped working after IBAMA inspection operations in Rorainópolis (G1, 2018a) and in the port of Manaus, Amazonas (G1, 2018b). In addition, it supports the supposition that permits for SL in areas released for "alternative land use" (deforestation) are used to launder wood.

4.3. Wood laundering as a factor in selective logging and consequent fire

While the 2015–2016 El Niño provided ideal climatic conditions for fires (Aragão et al., 2018; Burton et al., 2020; Fonseca et al., 2017; Ray et al., 2005), much of the "blame" for the fires and the damage they caused can be attributed to the roles of SL in increasing the probability of areas being burned and in increasing the damage when burning occurs. The large area of selective logging in our study area appears to be mainly the result of permits from authorized deforestation being used to provide cover for transporting the logs to sawmills (i.e., "laundering" wood) and a lesser amount from authorized forest-management projects.

In our study area logging is done based on the approval of licenses for clearing forest for agriculture and pasture. In these projects FEMARH authorizes the sale of a restricted volume of wood, which generally varies between 20 and 100 m^3 per ha of authorized clearing (e.g., Barni et al., 2020). These authorizations are often used to "launder" wood from illegal logging in nearby forests, including wood from outside of the properties where the clearcutting was licensed (Condé et al., 2019). In these clearcutting projects, the wood is harvested before the forest is cleared, and one to two years or more (See table S3) elapse before the remaining trees are cut when the area is deforested for pasture (this is recurrent throughout the southern portion of the state). In this case, the forest contains large clearings resulting from the opening of roads and log-storage yards, with the remaining trees left standing until the end of

Table 7
Effect of logging on area and biomass burned.

	A	B	C	D	E	F	G	H	I
Forest type	Total area burned (km^2)	Area burned w/SL (km^2)	Area burned that would have remained unburned w/o SL (km^2)	Average biomass w/SL (Mg ha^{-1})	Fraction Killed by fire W/SL	Average biomass killed by fire in burned area that would have remained unburned w/o SL (Mg ha^{-1})	Total biomass killed by fire in burned area that would have remained unburned (10^6 Mg)	Fraction killed by fire Wo/SL	Area that would have burned if there had been no SL in areas that had SL (km^2)
Source	Table 6	Table 6	B - I	Table 4	Table 5	D × E	C × 100 × F/10^6	Table 6	B - C
Ombrophilous	532.7	152.3		399.6	0.232	92.6		0.216	
Campinarana	140.0	28.3		230.3	0.232	61.0		0.218	
Ecotone	9.3							0.194	
All types	681.9	180.6	138.4	384.2	0.232	89.1	1.22	0.216	43.4
	J	K	L	M	N	O	P	Q	R
	Additional fraction burned W/SL as compared to Wo/SL	Average additional biomass killed by fire in area W/SL that would have burned w/o SL (Mg ha^{-1})	Total additional biomass killed by fire in area W/SL that would have burned w/o SL (10^6 Mg)	Total additional biomass killed by fire due to SL (10^6 Mg)	Fraction of original biomass removed or killed by SL	Average biomass Wo/SL (Mg ha^{-1})	Average biomass removed or killed by SL (Mg ha^{-1})	Total biomass removed or killed by SL in study area w/SL (10^6 Mg)	Percent increase of impact of SL due to additional area burned (%)
Source	E - H	D × S	((B-D) × 100-T) /10^6	G + U	Section 2.3.2	Table 6	W × X	T × 100 × Y /10^6	V/Z × 100
Ombrophilous	0.016	6.4			0.082	435.0	35.7	0.54	
Campinarana	0.014	3.1			0.082	250.8	20.6	0.06	
Ecotone						360.3			
All types	0.016	6.0	0.03	1.25	0.082	395.0	32.3	1.69	74.1
	S	T	U	V	W	X			
	Total area present (km^2)	Total area logged (km^2)	Total area not logged (km^2)	Total area burned w/SL (km^2)	Total area burned wo/SL (km^2)	Total area burned (km^2)			
Source	Table S-13	Section 4.2.2	S - T	Table 6	Table 6	V + W			
Ombrophilous	5,720.8			152.3	380.3	532.7			
Campinarana	727.9			28.3	111.7	140.0			
Ecotone	63.7					9.3			
All types	6,512.4	520.5	5,991.9	180.6	501.3	681.9			
	Y	Z	AA	AB	AC	AD			
	Percent burned of area logged (%)	Percent burned of area not logged (%)	Area that would have burned in logged area if unlogged (km^2)	Loss from fire due to logging effect on burned area as % of loss from logging (%)	Total biomass loss from fire due to logging (10^6 Mg)	Biomass loss from fire due to logging as % of loss from logging (%)			
Source	V/T ×100	W/U ×100	Z/100 × AJ	G/Q × 100	G + M	AC/Q × 100			
All types	34.7	8.4	43.5	72.5	2.47	146.5			

the logging operation before being cut. The burning of areas that are deforested in clearcutting projects serve as sources of ignition for the spread of fire to the adjacent forest. Logging disturbance can be more serious than the deforestation itself as a force for spreading fire. Under extreme climatic conditions such as the 2015/2016 El Niño event (Burton et al., 2020; Fonseca et al., 2017), logged areas become highly vulnerable to fires (Andrade et al., 2020; Cochrane et al., 1999; de Faria et al., 2017; Morton et al., 2011; Ziccardi et al., 2019). The logged areas served as "springboards" for fire to gain momentum and spread to adjacent areas, including those without evidence of SL.

This effect of recent logging was shown by the correlation analysis between the incidence of fire and the difference between the NDVI values observed in SL areas carried out in years immediately before the fires and the NDVI values observed in the same places in 2016 (Figure S9). The increasing correlation between these values over time is consistent with the more recently logged areas having greater fire severity (Fig. 5B). This corroborates the studies by (Souza Jr. et al., 2005a, 2005b, 2013), who analyzed forest degradation by SL and fire using multitemporal images.

4.4. Vulnerability of the forest to understory fires

The variables that contributed the most to the vulnerability of the forest were, in decreasing order, the distance from secondary roads, the distance from previous or cumulative deforestation and the distance from selective logging. The effects of major and secondary roads on the occurrence of deforestation and forest fires in the Amazon are well known (Barni et al., 2015b; Fonseca et al., 2017, 2019; Silvestrini et al., 2011; Soares-Filho et al., 2006). However, with regard to modeling the risk of forest fire using SL as an explanatory variable in the model, our results are unprecedented and demonstrate the importance of regulating this activity for combating and controlling forest fires in Brazilian Amazonia.

Modeling the probability of the occurrence of fires in the study area using the weights-of-evidence method allowed us to produce a vulnerability map of the forest (map with all variables) with very high spatial resolution (compatible with the Landsat 8 pixel size of 30 m). Providing information for use in risk maps for the occurrence of catastrophic events, such as floods, hurricanes and forest fires, is valuable for planning and for preventing and mitigating the potential impacts these calamities cause to the economic, social and environmental sectors. Increasing the accuracy of models can make them more effective as a basis for public policies to reduce these risks (Ferrier et al., 2016; Fonseca et al., 2017, 2019; Marcelino, 2008). The map of forest vulnerability to fire modeled in this study can serve as a tool for planning preventive measures for combating fires and for mitigating the effects of fire in Roraima (Barbosa et al., 2003). The increased vulnerability of selectively logged forest to fire implies that the simple assumption that authorized forest management projects in Amazonia are sustainable is unwarranted. One cannot simply assume that if government regulations on the intensity of logging and other factors in management systems are followed then the system will automatically be sustainable. Unfortunately, fire was not considered in the forest-recovery studies underlying official regulations. Virtually all plans for forest management in Amazonia assume that the managed areas will never burn (see Fearnside, 2003). The falseness of this assumption is central to discussions of the appropriate role of forest management in Amazonian development.

The roles of selective logging in facilitating forest fires and increasing their damage mean that SL can have harmful and unpredictable consequences for the structure of the forest (Rappaport et al., 2018). Fires also affect the forest's health, with repercussions for the survival of arboreal individuals in the years following the fires (Andrade et al., 2020; Trumbore et al., 2015; Watson et al., 2018; Ziccardi et al., 2019). The increase in fire severity provoked by logging implies direct impacts on greenhouse-gas emissions and global climate (Aragão et al., 2007, Assis et al., 2020; de Faria et al., 2017; Rappaport et al., 2018; Stark et al., 2020; Trumbore et al., 2015). Fires like these are known to initiate a positive-feedback process, where the fire leaves dead wood in the forest that serves as fuel for the next fire at the time of another extreme drought event, making this and subsequent fires more intense, and this can completely destroy an area of forest after three or four fires (Berenguer et al., 2014; Cochrane et al., 1999; Nepstad et al., 1999). The effect of fire in more than doubling the impact of the logging itself, increasing the impact by 146.5%, affects the calculus for forest management. This level of impact is the result of a single fire, and this is only the beginning of the positive feedback process of degradation in a downward spiral of biomass stocks. The large impact of selective logging through the effect on fire should both serve as a warning to policy makers promoting forest management and add urgency to repressing the widespread illegal logging in Amazonia.

5. Conclusions

The methods developed here to estimate the effects of selective logging based on fire-severity classes and the modeling of fire spread based on weights-of-evidence can be used as a tool for creating public policies regarding logging and fire. The results these policies need to be more cautious in promoting forest management and more rigorous in controlling illegal logging, as well as increasing efforts to prevent fires.

The selective logging practiced in the southern portion of Roraima contributed significantly to the increase in damage to forest biomass and consequent emission of carbon to the atmosphere, in addition to facilitating the spreading of forest fires and increasing their intensity. If a hectare of forest is burned, the fire intensity is 85.9% more likely to be in the "very strong" category if it had been previously logged. Fire increased the impact of logging on biomass reduction by 146.5% as compared to the impact of the logging itself, thus more than doubling the impact of logging with just one fire. These results cast doubt on the assumption that approved forest-management projects are sustainable on the long term. In addition, the connection of logging disturbance and resulting forest fires to authorized wood sales from areas licensed for clearcutting indicates the need for Roraima's environmental agency (FEMARH) to revise its policies on the use of wood from forest-clearing projects.

CRediT authorship contribution statement

Paulo Eduardo Barni: Conceptualization, Writing-original draft, Methodology, Data curation, Project administration, Resources, Software, Formal analysis, Validation. **Anelícia Cleide Martins Rego:** Investigation. **Francisco das Chagas Ferreira Silva:** Investigation. **Richard Anderson Silva Lopes:** Writing - review & editing. **Haron Abrahim Magalhães Xaud:** Writing - review & editing. **Maristela Ramalho Xaud:** Writing - review & editing. **Reinaldo Imbrozio Barbosa:** Data curation, Methodology, Writing - review & editing, Formal analysis, Validation. **Philip Martin Fearnside:** Data curation, Methodology, Writing - review & editing, Formal analysis, Resources, Software, Funding acquisition, Supervision, Validation.

Declaration of Competing Interest

The authors declare that they have no known competing financial interests or personal relationships that could have appeared to influence the work reported in this paper.

Acknowledgments

A.C.M. Rego participated as a volunteer in the Institutional Program for Scientific Initiation Scholarships (PIBIC) of the National Council for Scientific and Technological Development (CNPq) in PIBIC Call No. 1/2018 of the project "Dynamics of Selective Logging – SL in the southern portion of the State of Roraima from 2007 to 2018." CNPq also provided

fellowships for P.M. Fearnside (Proc. 311103/2015-4) and R.I. Barbosa (Proc. 304204/2015-3). This paper is a contribution of the Brazilian Research Network on Global Climate Change FINEP/Rede CLIMA Grant 01.13.0353-00. We thank the State Foundation for the Environment and Water Resources (FEMARH) for providing valuable data on selective logging.

Appendix A. Supplementary material

Supplementary data to this article can be found online at https://doi.org/10.1016/j.foreco.2021.119652.

References

Alencar, A., Nepstad, D., Diaz, M.D.V., 2006. Forest understory fire in the Brazilian Amazon in ENSO and non-ENSO years: Area burned and committed carbon emissions. Earth Interact 10 (6). https://doi.org/10.1175/EI150.1.

Alencar, A.A., Brando, P.M., Asner, G.P., Putz, F.E., 2015. Landscape fragmentation, severe drought and the new Amazon forest fire regime. Ecol. Appl. 25 (6), 1493–1505. https://doi.org/10.1890/14-1528.1.

Alvares, C.A., Stape, J.L., Sentelhas, P.C., de Moraes Gonçalves, J.L., Sparovek, G., 2014. Köppen's climate classification map for Brazil. Meteorol. Z. 22 (6), 711–728. https://doi.org/10.1127/0941-2948/2013/0507.

Andrade, D.F.C., Ruschel, A.R., Schwartz, G., de Carvalho, J.O.P., Humphries, S., Gama, J.R.V., 2020. Forest resilience to fire in eastern Amazon depends on the intensity of prefire disturbance. art. 118258 For. Ecol. Manage. 472. https://doi.org/10.1016/j.foreco.2020.118258.

Aragão, L.E.O.C., Malhi, Y., Roman-Cuesta, R.M., Saatchi, S., Anderson, L.O., Shimabukuro, Y.E., 2007. Spatial patterns and fire response of recent Amazonian droughts. art. L07701 Geophys. Res. Lett. 34 (7). https://doi.org/10.1029/2006GL028946.

Aragao, L.E.O.C., Shimabukuro, Y.E., 2010. The incidence of fire in Amazonian forests with implications for REDD. Science 328 (5983), 1275–1278. https://doi.org/10.1126/science:1186925.

Aragão, L.E.O.C., Anderson, L.O., Fonseca, M.G., Rosan, T.M., Vedovato, L.B., Wagner, F. H., Silva, C.V.J., Silva Junior, C.H.L., Arai, E., Aguiar, A.P., Barlow, J., Berenguer, E., Deeter, M.N., Domingues, L.G., Gatti, L., Gloor, M., Malhi, Y., Marengo, J.A., Miller, J.B., Phillips, O.L., Saatchi, S., 2018. 21st Century drought-related fires counteract the decline of Amazon deforestation carbon emissions. Nat. Commun. 9 (1) https://doi.org/10.1038/s41467-017-02771-y.

Assis, T.O., Aguiar, A.P.D., von Randow, C., Gomes, D.M.P., Kury, J.N., Ometto, J.P.H.B., Nobre, C.A., 2020. CO_2 emissions from forest degradation in Brazilian Amazonia. art. 104035 Environ. Res. Lett. 15 (10). https://doi.org/10.1088/1748-9326/ab9cfc.

Baccini, A., Goetz, S.J., Walker, W.S., Laporte, N.T., Sun, M., Sulla-Menashe, D., Hackler, J., Beck, P.S.A., Dubayah, R., Friedl, M.A., Samanta, S., Houghton, R.A., 2012. Estimated carbon dioxide emissions from tropical deforestation improved by carbon-density maps. Nat. Clim. Change 2 (3), 182–185. https://doi.org/10.1038/nclimate1354.

Barbosa, R.I., Fearnside, P.M., 1999. Incêndios na Amazônia: Estimativa da emissão de gases de efeito estufa pela queima de diferentes ecossistemas de Roraima na passagem do evento El-Niño (1997/1998). Acta Amazonica 29 (4), 513–534. https://doi.org/10.1590/1809-43921999294534.

Barbosa, R.I., Xaud, M.R., Silva, G.N.F., Cattâneo, A.C., 2003. Forest Fires in Roraima, Brazilian Amazonia. International Forest Fire News (IFFN) 28, 51–56. https://gfmc.online/wp-content/uploads/Brazil-2-1.pdf.

Barni, P.E., Silva, E.B.R., 2017. Extração seletiva de madeira em Rorainópolis: A floresta em perigo. In: Anais da Semana Nacional de Ciência e Tecnologia no estado de Roraima: Ciência alimentando Brasil. Universidade Estadual de Roraima (UERR), Boa Vista, RR. art. 36103. https://bityl.co/5JbX. Accessed on: 23 January 2021.

Barni, P.E., Silva, E.B.R., Silva, F.C.F., 2017. Incêndios florestais de sub-bosque na zona de florestas úmidas do sul de Roraima: Área atingida e biomassa morta. In: Anais do Simpósio Brasileiro de Sensoriamento Remoto 2017. Campinas, SP, Brazil: Galoá, pp. 6280-6287. Available at: https://bityl.co/5JeV. Accessed on: 21 November 2020.

Barni, P.E., Pereira, V.B., Manzi, A.O., Barbosa, R.I., 2015a. Deforestation and forest fires in Roraima and their relationship with phytoclimatic regions in the northern Brazilian Amazon. Environ. Manage. 55 (5), 1124–1138. https://doi.org/10.1007/s00267-015-0447-7.

Barni, P.E., Fearnside, P.M., Graça, P.M.L.A., 2015b. Simulating deforestation and carbon loss in Amazonia: Impacts in Brazil's Roraima state from reconstructing Highway BR-319 (Manaus-Porto Velho). Environ. Manage. 55 (2), 259–278. https://doi.org/10.1007/s00267-014-0408-6.

Barni, P.E., Manzi, A.O., Condé, T.M., Barbosa, R.I., Fearnside, P.M., 2016. Spatial distribution of forest biomass in Brazil's state of Roraima, northern Amazonia. For. Ecol. Manage. 377, 170–181. https://doi.org/10.1016/j.foreco.2016.07.010.

Barni, P.E., Barbosa, R.I., Manzi, A.O., Fearnside, P.M., 2020. Simulated deforestation versus satellite data in Roraima, northern Amazonia. Brazil. Sustentabilidade em Debate 11 (2), 81–94. https://doi.org/10.18472/SustDeb.v11n2.2020.27493.

Bastarrika, A., Chuvieco, E., Martín, M.P., 2011. Automatic burned land mapping from MODIS time series images: assessment in Mediterranean ecosystems. IEEE Trans. Geosci. Remote Sens. 49 (9), 3401–3413. https://doi.org/10.1109/TGRS.2011.2128327.

Berenguer, E., Ferreira, J., Gardner, T.A., Aragão, L.E.O.C., De Camargo, P.B., Cerri, C.E., Durigan, M., Oliveira, R.C.D., Vieira, I.C.G., Barlow, J., 2014. A large-scale field assessment of carbon stocks in human-modified tropical forests. Glob. Change Biol. 20 (12), 3713–3726. https://doi.org/10.1111/gcb.12627.

Bonham-Carter, G., 1994. Geographic Information Systems for Geoscientists: Modeling with GIS. Pergamon, New York, USA, p. 398.

Brancalion, P.H.S., de Almeida, D.R.A., Vidal, E., Molin, P.G., Sontag, V.E., Souza, S.E.X. F., Schulze, M.D., 2018. Fake legal logging in the Brazilian Amazon. Sci. Adv. 4 (8), eaat1192. https://doi.org/10.1126/sciadv.aat1192.

Brando, P.M., Balch, J.K., Nepstad, D.C., Morton, D.C., Putz, F.E., Coe, M.T., Silvério, D., Macedo, M.N., Davidson, E.A., Nóbrega, C.C., Alencar, A., Soares-Filho, B.S., 2014. Abrupt increases in Amazonian tree mortality due to drought–fire interactions. Proc. Natl. Acad. Sci. USA 111 (17), 6347–6352. https://doi.org/10.1073/pnas.1305499111.

Brando, P.M., Paolucci, L., Ummenhofer, C.C., Ordway, E.M., Hartmann, H., Cattau, M. E., Rattis, L., Medjibe, V., Coe, M.T., Balch, J., 2019. Droughts, wildfires, and forest carbon cycling: A pantropical synthesis. Annu. Rev. Earth Planet. Sci. 47 (1), 555–581. https://doi.org/10.1146/annurev-earth-082517-010235.

Brazil, IBGE (Instituto Brasileiro de Geografia e Estatística), 2021. Produção da Extração Vegetal e da Silvicultura: Tabela 289. Available at: https://sidra.ibge.gov.br/Tabela/289. Accessed on: 19 March 2021.

Brazil, INPE (Instituto Nacional de Pesquisas Espaciais), 2020. Projeto PRODES – Monitoramento da Floresta Amazônica por Satélite. São José dos Campos, SP, Brazil: INPE. Available at: https://bityl.co/5JeS. Accessed on: 21 November 2020.

Brazil, MCTI (Ministério da Ciência, Tecnologia e Inovação), 2020. Estimativas Anuais de Emissões de Gases de Efeito Estufa no Brasil. Quinta edição. 108 pp., Available at: https://bityl.co/5JeH. Accessed on: 21 November 2020.

Brazil, PROBio (Projeto da Biodiversidade Brasileira), 2013. Mapas de Cobertura Vegetal dos Biomas Brasileiros. Available at: https://bityl.co/5JeR. Accessed on: 21 November 2020.

Brazil, RADAMBRASIL, 1973–1983. Levantamento dos Recursos Naturais (Folhas SA.20 Manaus; SA.21 Santarém; SB.19 Juruá; SB.20 Purus; SC.19 Rio Branco; SC.20 Porto Velho). Rio de Janeiro, RJ, Brazil: Ministério das Minas e Energia.

Broadbent, E.N., Asner, G.P., Keller, M., Knapp, D.E., Oliveira, P.J.C., Silva, J.N., 2008. Forest fragmentation and edge effects from deforestation and selective logging in the Brazilian Amazon. Biol. Conserv. 141 (7), 1745–1757. https://doi.org/10.1016/j.biocon.2008.04.024.

Burton, C., Betts, R.A., Jones, C.D., Feldpausch, T.R., Cardoso, M., Anderson, L.O., 2020. El Niño driven changes in global fire 2015/16. Front. Earth Sci. 8, 1–12. https://doi.org/10.3389/feart.2020.00199.

Chuvieco, E., Martín, M.P., Palacios, A., 2002. Assessment of different spectral indices in the red-near infrared spectral domain of burned land discrimination. Int. J. Remote Sens. 23, 5103–5110. https://doi.org/10.1080/01431160210153129.

Cochrane, M.A., Alencar, A., Schulze, M., Souza Jr., C., Nepstad, D.C., Lefebvre, P., Davidson, E., 1999. Positive feedbacks in the fire dynamic of closed canopy tropical forests. Science 284, 1832–1835. https://doi.org/10.1126/science.284.5421.1832.

Cohen, J., 1988. Statistical power analysis for the behavioral sciences. Hillsdale, NJ, USA: Erlbaum. Available at: http://www.utstat.toronto.edu/~brunner/oldclass/378f16/readings/CohenPower.pdf. Accessed on: 2 April 2021.

Condé, T.M., Higuchi, N., Lima, A.J.N., 2019. Illegal selective logging and forest fires in the northern Brazilian Amazon. Forests 10, art. 61. https://doi.org/10.3390/f10010061.

Crivelli, B.R.S., Gomes, J.P., Morais, W.W.C., Condé, T.M., Santos, R.L., Bonfim Filho, O. S., 2017. Caracterização do setor madeireiro de Rorainópolis, sul de Roraima. Revista Ciência da Madeira 8 (3), 142–150.

da Silva, S.S., Fearnside, P.M., Graça, P.M.L.A., Brown, I.F., Alencar, A., de Melo, A.W.F., 2018. Dynamics of forest fires in the southwestern Amazon. For. Ecol. Manage. 424, 312–322. https://doi.org/10.1016/j.foreco.2018.04.041.

de Faria, B.L., Brando, P.M., Macedo, M.N., Panday, P.K., Soares-Filho, B.S., Coe, M.T., 2017. Current and future patterns of fire-induced forest degradation in Amazonia. Environ. Res. Lett. 12 (9), 1–13. https://doi.org/10.1088/1748-9326/aa69ce.

Dent, B.D., Torguson, J., Hodler, T., 1990. Cartography: Thematic Map Design, Second edition. William C. Brown, Dubuque, IA, p. 448.

Fearnside, P.M., 1997. Wood density for estimating forest biomass in Brazilian Amazonia. For. Ecol. Manage. 90 (1), 59–89. https://doi.org/10.1016/S0378-1127(96)03840-6.

Fearnside, P.M., 2003. Conservation policy in Brazilian Amazonia: Understanding the dilemmas. World Dev. 31 (5), 757–779. https://doi.org/10.1016/S0305-750X(03)00011-1.

Fearnside, Philip M., 2008. Amazon forest maintenance as a source of environmental services. Anais da Academia Brasileira de Ciências 80 (1), 101–114. https://doi.org/10.1590/S0001-37652008000100006.

Fearnside, P.M., Barbosa, R.I., Pereira, V.B., 2013. Emissões de gases do efeito estufa por desmatamento e incêndios florestais em Roraima: Fontes e sumidouros. Revista Agroambiente On-line 7, 95–111. https://doi.org/10.18227/1982-8470ragro.v7i1.971.

Fernández-Manso, A., Fernández-Manso, O., Quintano, C., 2016. SENTINEL-2A red-edge spectral indices suitability for discriminating burn severity. Int. J. Appl. Earth Obs. Geoinf. 50, 170–175. https://doi.org/10.1016/j.jag.2016.03.005.

Ferrante, L., Fearnside, P.M., 2019. Brazil's new president and "ruralists" threaten Amazonia's environment, traditional peoples and the global climate. Environ. Conserv. 46 (4), 261–263. https://doi.org/10.1017/S0376892919000213.

Fonseca, M.G., Anderson, L.O., Arai, E., Shimabukuro, Y.E., Xaud, H.A.M., Xaud, M.R., Madani, N., Wagner, F.H., Aragão, L.E.O.C., 2017. Climatic and anthropogenic drivers of northern Amazon fires during the 2015–2016 El Niño event. Ecol. Appl. 27 (8), 2514–2527. https://doi.org/10.1002/eap.1628.

Fonseca, M.G., Alves, L.M., Aguiar, A.P.D., Arai, E., Anderson, L.O., Rosan, T.M., Shimabukuro, Y.E., Aragão, L.E.O.C., 2019. Effects of climate and land-use change scenarios on fire probability during the 21st century in the Brazilian Amazon. Glob. Change Biol. 25 (9), 2931–2946. https://doi.org/10.1111/gcb.v25.910.1111/gcb.14709.

Ferrier, S., Ninan, K.N., Leadley, P., Alkemade, R., Acosta, L.A., Akçakaya, H.R., Brotons, L., Cheung, W.W.L., Christensen, V., Harhash, K.A., Kabubo-Mariara, J., Lundquist, C., Obersteiner, M., Pereira, H.M., Peterson, G., Pichs-Madruga, R., Ravindranath, N., Rondinini C., Wintle B.A. (Eds.), 2016. IPBES: The methodological assessment report on scenarios and models of biodiversity and ecosystem services. Bonn, Germany. Secretariat of the Intergovernmental Science-Policy Platform on Biodiversity and Ecosystem Services, 348 pp. https://ipbes.net/assessment-reports/scenarios.

G1, 2018a. Protesto contra fechamento de madeireiras interdita rodovia em Rorainópolis, Sul de RR. Available at: https://bityl.co/7EMh. Accessed on: 26 January 2021.

G1, 2018b. PF faz operação de combate à exploração ilícita de madeira da Amazônia. Available at: https://bityl.co/5Jdo. Accessed on: 21 November 2020.

Gimenez, B.O., Danielli, F.E., Oliveira, C.K.A., Santos, J., Higuchi, N., 2015. Equações volumétricas para espécies comerciais madeireiras do sul do estado de Roraima. Scientia Forestales 43, 291–301. https://www.ipef.br/publicacoes/scientia/nr106/cap05.pdf.

Hagen, Alex, 2003. Fuzzy set approach to assessing similarity of categorical maps. Int. J. Geographical Inform. Sci. 17 (3), 235–249. https://doi.org/10.1080/13658810210157822.

Hethcoat, M.G., Carreiras, J.M.B., Edwards, D.P., Bryant, R.G., Peres, C.A., Quegan, S., 2020. Mapping pervasive selective logging in the south-west Brazilian Amazon 2000–2019. art. 094057 Environ. Res. Lett. 15. https://doi.org/10.1088/1748-9326/aba3a4.

Higuchi, N., Santos, J., Ribeiro, R.J., Minette, L., Biot, Y., 1998. Biomassa da parte aérea da vegetação da floresta tropical úmida de terra-firme da Amazônia brasileira. Acta Amazonica 28 (2), 153–166. https://doi.org/10.1590/1809-43921998282166.

Jiménez-Muñoz, J.C., Mattar, C., Barichivich, J., Santamaría-Artigas, A., Takahashi, K., Malhi, Y., et al., 2016. Record-breaking warming and extreme drought in the Amazon rainforest during the course of El Niño 2015–2016. Sci. Rep. 6 (1) https://doi.org/10.1038/srep33130.

Leite-Filho, A.T., Soares-Filho, B.S., Davis, J.L., Abrahão, G.M., Börner, J., 2021. Deforestation reduces rainfall and agricultural revenues in the Brazilian Amazon. Nat. Commun. 12, art. 2591. https://doi.org/10.1038/s41467-021-22840-7.

Lentini, M., Pereira, D., Celentano, D., Pereira, R., 2005. Fatos florestais da Amazônia 2005. Belém, PA, Brazil: Instituto do Homem e Meio Ambiente da Amazônia (Imazon). 140 pp. https://bityl.co/5JdR.

Marcelino, E.V., 2008. Desastres Naturais e Geotecnologias: Conceitos Básicos. Caderno Didático n° 1. Santa Maria, RS, Brazil: CRS, Instituto Nacional de Pesquisas Espaciais (INPE), 38 pp. https://bityl.co/5JdF.

McLauchlan, K.K., Higuera, P.E., Miesel, J., Rogers, B.M., Schweitzer, J., Shuman, J.K., Tepley, A.J., Varner, J.M., Veblen, T.T., Adalsteinsson, S.A., et al., 2020. Fire as a fundamental ecological process: Research advances and frontiers. J. Ecol. 108 (5), 2047–2069. https://doi.org/10.1111/jec.v108.510.1111/1365-2745.13403.

Meira-Junior, M.S., Pinto, J.R.R., Ramos, N.O., Miguel, E.P., Gaspar, R.O., Phillips, O.L., 2020. The impact of long dry periods on the aboveground biomass in a tropical forest: 20 years of monitoring. Carbon Balance Manage. 15, art. 12. https://doi.org/10.1186/s13021-020-00147-2.

Monteiro, A., Cardoso, D., Conrado, D., Veríssimo, A., Souza Jr, C., 2010. Boletim Transparência Manejo Florestal- Estado do Pará 2008 a 2009. Belém, PA, Brazil: Instituto do Homem e Meio Ambiente da Amazônia (Imazon), 16 pp. https://bityl.co/5Jd4.

Morton, D.C., DeFries, R.S., Nagol, J., Souza Jr., C.M., Kasischke, E.S., Hurtt, G.C., Dubayah, R., 2011. Mapping canopy damage from understory fires in Amazon forests using annual time series of Landsat and MODIS data. Remote Sens. Environ. 115 (7), 1706–1720. https://doi.org/10.1016/j.rse.2011.03.002.

Nepstad, D.C., Veríssimo, A., Alencar, A., Nobre, C., Lima, E., Lefebvre, P., Schlesinger, P., Potter, C., Moutinho, P., Mendoza, E., Cochrane, M., Brooks, V., 1999. Large-scale impoverishment of Amazonian forests by logging and fire. Nature 398, 505–508. https://www.nature.com/articles/19066.

Nepstad, D., Lefebvre, P., Lopes da Silva, U., Tomasella, J., Schlesinger, P., Solorzano, L., Moutinho, P., Ray, D., Guerreira Benito, J., 2004. Amazon drought and its implications for forest flammability and tree growth: A basin-wide analysis. Glob. Change Biol. 10 (5), 704–717. https://doi.org/10.1111/j.1529-8817.2003.00772.x.

Nepstad, D.C., Tohver, I.M., Ray, D., Moutinho, P., Cardinot, G., 2007. Mortality of large trees and lianas following experimental drought in an Amazon forest. Ecology 88 (9), 2259–2269. https://doi.org/10.1890/06-1046.1.

Nogueira, Euler Melo, Nelson, Bruce Walker, Fearnside, Philip M., 2005. Wood density in dense forest in central Amazonia, Brazil. For. Ecol. Manage. 208 (1-3), 261–286. https://doi.org/10.1016/j.foreco.2004.12.007.

Nogueira, E.M., Fearnside, P.M., Nelson, B.W., Barbosa, R.I., Keizer, E.W.H., 2008. Estimates of forest biomass in the Brazilian Amazon: New allometric equations and adjustments to biomass from wood-volume inventories. For. Ecol. Manage. 256 (11), 1853–1867. https://doi.org/10.1016/j.foreco.2008.07.022.

Oliveira, S., 2021. Rorainópolis, em RR, entra na lista de municípios com prioridade no controle ao desmatamento na Amazônia. G1, 13 January 2021. Available at: https://bityl.co/5Jdh. Accessed on: 15 January 2021.

Pereira, D., Santos, D., Vedoveto, M., Guimarães, J., Veríssimo, A., 2010. Fatos florestais da Amazônia. Belém, PA: Instituto do Homem e Meio Ambiente da Amazônia (Imazon), 124 pp. https://bityl.co/5Jd6.

Quintano, C., Fernández-Manso, A., Fernández-Manso, O., Shimabukuro, Y.E., 2006. Mapping burned areas in Mediterranean countries using spectral mixture analysis from a uni-temporal perspective. Int. J. Remote Sens. 27 (4), 645–662. https://doi.org/10.1080/01431160500212195.

Rappaport, D.I., Keller, M., Morton, D.C., Longo, M., Dubayah, R., Dos-Santos, M.N., 2018. Quantifying long-term changes in carbon stocks and forest structure from Amazon forest degradation. Environ. Res. Lett. 13 (6), 1–12. https://doi.org/10.1088/1748-9326/aac331.

Ray, D., Nepstad, D., Moutinho, P., 2005. Micrometeorological and canopy controls of fire susceptibility in a forested Amazon landscape. Ecol. Soc. Am. 15 (5), 1664–1678. https://doi.org/10.1890/05-0404.

Silva, C.V.J., Aragão, L.E.O.C., Barlow, J., Espirito-Santo, F., Young, P.J., Anderson, L.O., Berenguer, E., Brasil, I., Foster Brown, I., Castro, B., Farias, R., et al., 2018. Drought-induced Amazonian wildfires instigate a decadal scale disruption of forest carbon dynamics. Philosophical Trans. Roy. Soc. B 373 (1760), 20180043. https://doi.org/10.1098/rstb.2018.0043.

Silveira, L.H.C., Rezende, A.V., Vale, A.T., 2013. Teor de umidade e densidade básica da madeira de nove espécies comerciais amazônicas. Acta Amazonica 43 (2), 179–184. https://doi.org/10.1590/S0044-59672013000200007.

Silvestrini, R.A., Soares-Filho, B.S., Nepstad, D., Coe, M., Rodrigues, H., Assunção, R., 2011. Simulating fire regimes in the Amazon in response to climate change and deforestation. Ecol. Appl. 21 (5), 1573–1590. https://doi.org/10.1890/10-0827.1.

Slocum, T.A., 1999. Thematic Cartography and Visualization. Prentice Hall, Upper Saddle River, NJ, USA.

Soares-Filho, B.S., Nepstad, D.C., Curran, L.M., Cerqueira, G.C., Garcia, R.A., Ramos, C. A., Voll, E., McDonald, A., Lefebvre, P., Schlesinger, P., 2006. Modelling conservation in the Amazon basin. Nature 440 (7083), 520–523. https://doi.org/10.1038/nature04389.

Soares-Filho, B.S., Garcia, R.A., Rodrigues, H., Moro, S., Nepstad, D., 2008. Nexos entre as dimensões socioeconômicas e o desmatamento: A caminho de um modelo integrado. In: Batistella, M., Alves, D., Moran, E. (Eds.). Amazônia. Natureza e Sociedade em Transformação. v. 1., São Paulo, SP, Brazil: EDUSP. https://bityl.co/5Ji4.

Souza Jr., C.M., Roberts, D., Monteiro, A.L., 2005a. Multitemporal analysis of degraded forests in the southern Brazilian Amazon. Earth Interact 9, art. 19. https://doi.org/10.1175/EI132.1.

Souza Jr., C.M., Roberts, D., Cochrane, M.A., 2005b. Combining spectral and spatial information to map canopy damages from selective logging and forest fires. Remote Sens. Environ. 98, 329–343. https://doi.org/10.1016/j.rse.2005.07.013.

Souza Jr, C.M., Siqueira, J.V., Sales, M.H., Fonseca, A.V., Ribeiro, J.G., Numata, I., Cochrane, M.A., Barber, C.P., Roberts, D.A., Barlow, J., 2013. Ten-year Landsat classification of deforestation and forest degradation in the Brazilian Amazon. Remote Sens. 5 (11), 5493–5513. https://doi.org/10.3390/rs5115493.

Stark, S.C., Breshears, D.D., Aragón, S., Villegas, J.C., Law, D.J., Smith, M.N., Minor, D. M., de Assis, R.L., de Almeida, D.R.A., de Oliveira, G., Saleska, S.R., Swann, A.L.S., Moura, J.M.S., Camargo, J.L., da Silva, R., Aragão, L.E.O.C., Oliveira, R.C., 2020. Reframing tropical savannization: Linking changes in canopy structure to energy balance alterations that impact climate. art. e03231 Ecosphere 11 (9). https://doi.org/10.1002/ecs2.3231.

Stroppiana, D., Bordogna, G., Carrara, P., Boschetti, M., Boschetti, L., Brivio, P.A., 2012. A method for extracting burned areas from Landsat TM/ETM+ images by soft aggregation of multiple Spectral indices and a region growing algorithm. ISPRS J. Photogramm. Remote Sens. 69 (1), 88–102. https://doi.org/10.1016/j.isprsjprs.2012.03.001.

Trumbore, S., Brando, P., Hartmann, H., 2015. Forest health and global change. Science 349 (6250), 814–818. https://doi.org/10.1126/science:aac6759.

Turubanova, S., Potapov, P.V., Tyukavina, A., Hansen, M.C., 2018. Ongoing primary forest loss in Brazil, Democratic Republic of the Congo, and Indonesia. Environ. Res. Lett. 13 (7), 074028. https://doi.org/10.1088/1748-9326/aacd1c.

Uhl, C., Buschbacher, R., 1985. A disturbing synergism between cattle-ranch burning practices and selective tree harvesting in the eastern Amazon. Biotropica 17 (4), 265–268. https://doi.org/10.2307/2388588.

USGS (U.S. Geological Survey), 2016. U.S. Department of the Interior, USGS. Available at: http://earthexplorer.usgs.gov/. Accessed on: 20 October 2016.

Watson, J.E.M., Evans, T., Venter, O., Williams, B., Tulloch, A., Stewart, C., Thompson, I., Ray, J.C., Murray, K., Salazar, A., et al., 2018. The exceptional value of intact forest ecosystems. Nat. Ecol. Evol. 2 (4), 599–610. https://doi.org/10.1038/s41559-018-0490-x.

West, T.A.P., Fearnside, P.M., 2021. Brazil's conservation reform and the reduction of deforestation in Amazonia. art. 105072 Land Use Policy 100. https://doi.org/10.1016/j.landusepol.2020.105072.

Xaud, H.A.M., Martins, F.S.R.V., Santos, J.R., 2013. Tropical forest degradation by mega-fires in the northern Brazilian Amazon. For. Ecol. Manage. 294, 97–106. https://doi.org/10.1016/j.foreco.2012.11.036.

Ziccardi, L.G., Graça, P.M.L.A., Figueiredo, E.O., Fearnside, P.M., 2019. Decline of large-diameter trees in a bamboo-dominated forest following anthropogenic disturbances in southwestern Amazonia. Ann. Forest Sci. 76, art. 110. https://doi.org/10.1007/s13595-019-0901-4.

Supplementary material

Logging Amazon forest increased the severity and spread of fires during the 2015-2016 El Niño

Paulo Eduardo Barni [1]
Anelícia Cleide Martins Rego [2]
Francisco das Chagas Ferreira Silva [2]
Richard Anderson Silva Lopes[3]
Haron Abrahim Magalhães Xaud [4]
Maristela Ramalho Xaud [4]
Reinaldo Imbrozio Barbosa [5]
Philip Martin Fearnside [6]

[1] Professor da Universidade Estadual de Roraima – UERR, *Campus* Rorainópolis
Av. Senador Helio Campos, s/nº, 69375-000, Rorainópolis, Roraima, Brazil.
pbarni@uerr.edu.br

[2] Graduados da Universidade Estadual de Roraima – UERR, *Campus* Rorainópolis
Av. Senador Helio Campos, s/nº, 69375-000, Rorainópolis, Roraima, Brazil.
{anelycia.com@gmail.com; chagasferreirasilva@gmail.com}

[3] Corpo de Bombeiros Militares de Roraima, Coordendoria Estadual de Proteção e Defesa Civil. Avenida Venezuela, 1271, 69309690 - Boa Vista, Roraima, Brazil.
{raslopes@gmail.com}

[4] Empresa Brasileira de Pesquisa Agropecuária – Embrapa/RR. Rodovia BR 174, Km 8, Distrito Industrial. 69301-970, Boa Vista, Roraima, Brazil. {haronxaud@gmail.com; marisxaud@gmail.com}

[5] Instituto Nacional de Pesquisas da Amazônia (INPA), Rua Coronel Pinto, 315. CEP: 69301-150. Boa Vista, Roraima, Brazil. reinaldo@inpa.gov.br

[6] Instituto Nacional de Pesquisas da Amazônia (INPA), Av. André Araújo, 2936. CEP: 69067-375, Manaus, Amazonas, Brazil. pmfearn@inpa.gov.br

Supplementary material index:

1. Methodological procedures

1.1 Study area

Most of the study area (6402.6 km^2, or 96.2% of the study area) is in the municipality of Rorainópolis, followed by the municipality of São Luiz (164.2 km^2, or 2.4%) and the municipality of Caracaraí (90.5 km^2, or 1.4 %) (Table S1).

Table S1. Deforestation, forest fire, and logging in the portion of each municipality located in the study area.

Municipalities	Area (km^2)	% of the study area	Deforestation km^2	%	Forest fire (km^2)	% of the burned area	SL (km^2)	% of the logged area
Caracaraí	90.5	1.4	7.1	0.6	37.9	5.6	9.4	1.5
Rorainópolis	6,402.6	96.2	1,045.3	94.8	638.3	93.6	624.4	96.8
São Luiz	164.2	2.4	49.7	4.5	6.0	0.9	10.9	1.7
Total	**6,657.3**	**100.0**	**1,102.1**	**100.0**	**682.2**	**100.0**	**644.8**	**100.0**

1.2 Forest inventory locations

The locations and other information for plots sampled in the field are presented in Table S2. All plots measured 4 × 250 m (1000 m^2).

Table S2. Location (latitude and longitude), area (ha) and date of field data collection. SL=Selective Logging. Wo-SL = without selective logging. W-SL = with selective logging.

Plot name	SL	Latitude	Longitude	Area (ha)	*AGB_stock (Mg ha^{-1})	Fire	Census date (mm/dd/yyyy)
Plot 1	W-SL	0.930891	-60.451279	0.1	404.6	yes	03/11/2016
Plot 2	W-SL	0.932695	-60.447959	0.1	221.5	yes	03/11/2016
Plot 3	W-SL	0.929629	-60.442604	0.1	458.5	yes	03/16/2016
Plot 4	W-SL	0.927556	-60.441827	0.1	322.0	yes	03/16/2016
Plot 5	W-SL	0.934315	-60.449995	0.1	640.2	yes	03/16/2016
Plot 6	W-SL	0.934234	-60.452384	0.1	834.0	yes	03/16/2016
Plot 7	W-SL	0.909708	-60.452814	0.1	320.1	yes	03/23/2016
Plot 8	W-SL	0.906816	-60.453078	0.1	567.2	yes	03/23/2016
Plot 9	W-SL	0.912540	-60.452564	0.1	1095.4	yes	03/23/2016
Plot 10	W-SL	0.913743	-60.454606	0.1	427.1	yes	03/23/2016
Plot 11	W-SL	0.711231	-60.565005	0.1	863.9	yes	03/30/2016
Plot 12	Wo-SL	0.707785	-60.510418	0.1	289.6	yes	03/30/2016
Plot 13	Wo-SL	0.709255	-60.508096	0.1	504.0	yes	03/30/2016
Plot 14	W-SL	0.709511	-60.567284	0.1	1044.2	yes	03/30/2016
Plot 15	W-SL	0.712057	-60.587902	0.1	387.6	yes	03/30/2016
Plot 16	W-SL	0.712389	-60.591582	0.1	424.0	yes	03/30/2016
Plot 17	Wo-SL	0.989933	-60.425055	0.1	546.6	yes	04/06/2016
Mean	-	-	-	-	**550.0**	-	-

*****Aboveground dry biomass stock based on Higuchi et al. (1998) with adjustment for 40% water content (Higuchi et al., 1998) and for biomass of palms (Saldarriaga et al., 1988).

1.3 Biomass calculation in inventory plots for deriving fractions of biomass killed

Unlike the biomass map for Roraima, which used the Barni et al. (2016) analysis with species specific data, only about half of the trees in the plots had known identities, and we therefore used the Higuchi et al. (1998) equation to calculate fresh biomass directly from DBH without using species-specific wood-density data. Because the plot data are only used for deriving the fractions of biomass killed by the fire in the different severity classes, not the forest

biomass to which these fractions will be applied, the use of different biomass estimation equations will not affect the results for the impact of fire in the study area, since the both the numerator and the dominator in the fractions of biomass killed have been calculated with the same method.

Fresh weight was converted to dry weight by multiplying by 0.60, which was the dry weight to fresh weight ratio derived by Higuchi et al. (1998: Table 3b). This rate was applied to the fresh-biomass value calculated by the Higuchi et al. (1998) equation for each tree in the database. This procedure was performed from the excel spreadsheet. Thus:

$$Ln(\text{Fresh weight}) = -1.497+2.548 \times Ln(DBH)$$
$$\text{Dry weight} = EXP(Ln(\text{Fresh weight})) \times 0.6$$

The total weight (kg^{-1}) of each plot (sum of the dry weight of all trees in the plot) was multiplied by 10 (to transform from kg^{-1} per plot to kg ha^{-1}) and, in sequence, the total weight in kg ha^{-1} was divided by 1000 to transform into Mg ha^{-1}.

1.4 Area (ha) and volume (m^3) authorized in "alternative land-use" projects

The largest area authorized for deforestation (3300.7 ha, or 26.4% of the total area authorized) was in 2015 and the smallest (290.6 ha, or 2.3%) was in 2011. Only 26.2% (3114.1 ha) of these areas authorized for alternative land use were effectively deforested by 2019 (Table S3).

Table S3. Area and volume of wood authorized for harvest in alternative land-use projects in the study area.

Year	n	Authorized area (ha)	Authorized volume (m^3)	Average volume (m^3 ha^{-1})	*Deforestation (ha)	%	**YARSL (n)
2010	9	2,095.4	133,939.0	63.7	525.9	25.1	2.8
2011	2	290.6	13,027.8	49.5	102.4	35.2	4
2012	17	3,244.9	150,319.5	50.6	755.5	23.3	2
2013	4	873.2	46,156.7	53.3	195.0	22.3	1
2014	12	2,676.1	114,311.9	43.0	695.8	26.0	1
2015	14	3,300.7	153,920.6	48.4	839.7	25.4	4
Total	**58**	**12,480.9**	**611,675.5**	**51.4**	**3114.1**	**26.2**	**2.5**

*** Deforestation by 2019.**
**** Years after the release to SL.**

1.5 "Sustainable Forest Management" Plans

The areas released for selective logging in "sustainable forest management" plans in Rorainópolis totaled 11,958.8 ha from 2016 to 2020 with an average authorized harvest of 23.9 m^3 ha^{-1}. In this area, a total volume of 281,091.3 m^3 of wood in logs was released (Table S4).

Table S4. Location (latitude and longitude), area (ha) and volume (m^3) authorized for logging in "sustainable forest management" plans in the municipality of Rorainópolis.

ID	Latitude	Longitude	Authorized area (ha)	Authorized volume (m^3)	Average volume (m^3 ha^{-1})	Year
1	0.4351889	-60.4069556	552.6	13,079.7	23.7	2019/20
2	0.3815278	-60.6354444	957.9	14,712.8	15.4	2017/18
3	0.5415483	-60.4245542	1,442.9	35,830.9	24.8	2019/20
4	0.7514861	-60.6653361	1,254.1	19,664.6	15.7	2018/19
5	0.5598333	-60.3416111	1,071.0	22,125.1	20.7	2018/19
6	0.7100000	-60.0663889	987.9	26,066.4	26.4	2016/17
7	0.5574109	-60.6592349	964.3	24,456.3	25.4	2020/21
8	0.2734927	-60.4002495	1,163.9	33,588.1	28.9	2020/21
9	0.5218820	-60.6587190	947.7	22,580.0	23.8	2020/21
10	0.9931272	-60.5705950	192.6	5.570.0	28.9	2020/21
11	0.2588300	-60.4437717	1,089.9	31,847.2	29.2	2020/21
12	0.4905078	-60.3520806	666.4	17,003.1	25.5	2020/21
13	0.4905078	-60.3520806	667.8	14,567.1	21.8	2020/21
Total			**11,958.8**	**281,091.3**	**23.9**	

1.6 Fire severity estimation by NDVI and NBR

The results of the comparison between NDVI and NBR using fire-severity classes (light, moderate, strong and very strong) are presented in Table S5. Figure S1 shows the results of the comparative analysis between the NDVI and the NBR in the assessment of burned areas. Figure S2 shows a portion of the study area with fire-severity classifications by each index.

The larger area that the NBR index detected in the lowest severity class (light), as compared to NDVI, is an indication in favor of NDVI as a more accurate index for our purposes. The fires in the area occurred from 1 December 2015 to 23 March 2016, with most of the 216 "hot pixels" detected by the Aqua satellite being detected between 15 January and 5 February 2016. This means that the bulk of the burning was almost five months before the satellite pass on 9 June 2016, and, with the rainy season beginning at the end of March, there were over two months of rain before the satellite pass. Therefore there had been time for regeneration of green vegetation in the understory of the burned areas. The burn-severity classification by the sensors would be most likely to downgrade the assignment of values in lower severity classes, such as classifying a "moderate" burn as "light," because the more-severe burns would inhibit regeneration. The close agreement between the two indices (9,6% NDVI and 8.6% NBR) in their findings for the highest severity class (very strong) can be explained by the almost total inhibition of regeneration in these places when fire is very intense. In this case, the intensity of the fire may have partially or totally eliminated the seed bank from the soil, thereby making more time necessary for regeneration (Figure S2).

NDVI and NBR use different bands, which may have made the green regeneration lead NBR to downgrade the assigned severities more than did NDVI. NDVI uses Landsat 8 sensor bands 5 (near infrared [NIR] wavelength range: 0.851 - 0.879 micrometers) and 4 (red: 0.636 - 0.673 micrometers). NBR uses bands 7 (short-wave infrared 2 [SWIR2]: 2.107 – 2.294 micrometers) and 5 (NIR: 0.851 - 0.879 micrometers). In the case of NBR, there is an increase in the contrast between the values of photosynthetically active vegetation and photosynthetically inactive vegetation (dead biomass). Higher reflectance levels associated with photosynthetically active vegetation, and part of this increase in "greenness" detected by NBR, can be attributed to forest regeneration by sprouting, seedling emergence from the soil seed bank and appearance of herbaceous plants in abundance.

Both indices capture the “greenness” effect, but this reflection is not very evident in the case of NDVI because this composition uses band 4 (red). When using band 7 to compose the NBR there is a greater expansion of the values due to the greater contrast (greater difference) between the reflection values of bands 5 and 7 than between the reflection values of bands 5 and 4 used to compose the NDVI. For example, in our study the range of the NBR index values was 0.5010 (0.7205 minus 0.2104: Table S5) while the range of the NDVI was 0.3784 (0.6031 minus 0.2247: Table 1 in the main text). This difference meant a 32.4% increase in the amplitude of the NBR values in relation to the amplitude of the NDVI values.

This explanation is speculative due to the lack of information linking ground-level regeneration with the NBR index. Our empirical experience suggests rapid regeneration in lower-severity burns. This subject should be the object of future studies in the region due to the importance of improving forest degradation estimates.

Table S5. Comparison analysis between NDVI and NBR using fire-severity classes.

	NDVI		**NBR**		**NDVI-NBR**		**NBR values**
Class	**Area (km^2)**	**%**	**Area (km^2)**	**%**	**Area (km^2)**	**%**	**Dimensionless (- 1 to +1)**
Light	245.8	36.2	282.9	41.7	-37.1	-15.1	0.5764 to 0.7205
Moderate	227.5	33.5	206.9	30.5	20.6	9.1	0.4904 to 0.5764
Strong	140.2	20.7	130.2	19.2	10.0	7.1	0.3944 to 0.4904
Very strong	64.8	9.6	58.3	8.6	6.5	10.0	0.2104 to 0.3944
Total	**678.3**	**100.0**	**678.3**	**100.0**	**0.0**	-	-

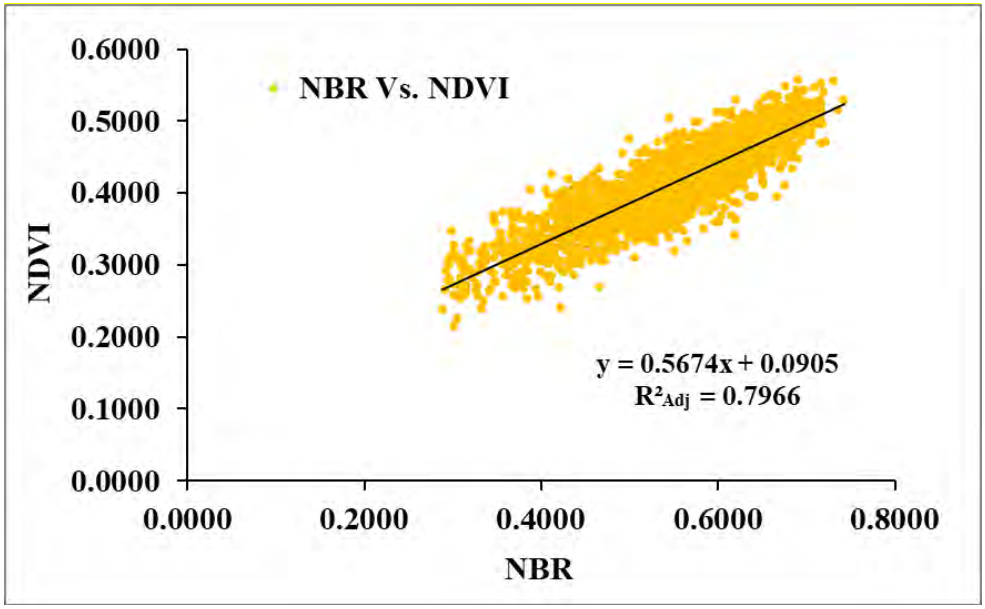

Figure S1. Comparison between sample values (n = 2502) for NBR and NDVI in burned areas in the study area.

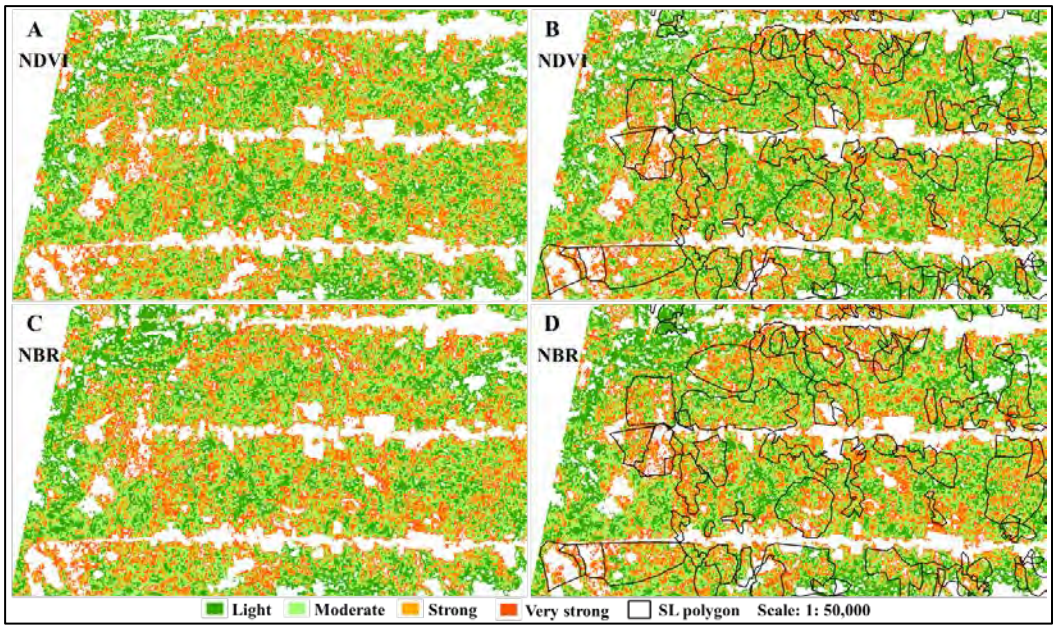

Figure S2. Fire severity classification using NDVI (A and B) and NBR (C and D) in a portion of the study area.

1.7 Wood density

The values calculated for the basic density of wood (g cm^{-3}) harvested in the SL areas are shown in Table S6. The table also provides the sources of the information.

Table S6. Calculation of weighted mean wood density.

Species	Local name	Wood volume (1)		Basic density	Note	Weighted	Density Source
		m^3	%	(g cm^{-3})			
Manilkara huberi	Maçaranduba	9,806	29.2	0.878	(2)	0.257	Silveira et al., 2013
Dinizia excelsa	Angelim-ferro	9,235	27.5	0.86		0.237	Fearnside, 1997
Hymenolobium excelsum	Angelim-pedra	4,440	13.2	0.64		0.085	Fearnside, 1997
Goupia glabra	Cupiúba	3,880	11.6	0.712	(2,3)	0.082	Nogueira et al., 2005
Erisma fuscum	Caferana	2,170	6.5	0.49	(4)	0.032	Fearnside, 1997
Qualea paraensis	Rabo-de-arraia	1,350	4.0	0.67		0.027	Fearnside, 1997
Protium sp.	Casca-grossa	1,000	3.0	0.589	(2,3,5)	0.018	Nogueira et al., 2005
Clarisia racemosa	Guaruba	1,000	3.0	0.665	(2)	0.020	Silveira et al., 2013
Couratari stellata	Tauari	320	1.0	0.63		0.006	Fearnside, 1997
Bagassa guianensis	Tatajuba	280	0.8	0.69		0.006	Fearnside, 1997
Handroanthus sp.	Ipê	77	0.2	0.91		0.002	Fearnside, 1997

(1) Wood volumes are from a 2013 survey of 9 sawmills in Rorainópolis by Crivelli et al., 2017).
(2) Includes variation along the trunk.
(3) Includes radial variation (density of cross-sectional discs, including bark)
(4) Density of a congeneric.
(5) Mean of 14 trees from 7 species.

1.8 Estimation of harvesting intensity and loss of live biomass from cumulative selective logging by 2015

Only an approximate value can be estimated for the loss of live biomass to selective logging at the time of the 2015-2016 fires. Official data on log volumes processed in sawmills and

authorized for sale have wide discrepancies, and data are only available for certain years for different measures (Table S7). The data for log volume processed in sawmills, which information is available for the most years (2007-2019) is particularly unreliable. From 2007 to 2014 the volume officially reported (Brazil, IBGE, 2021) averaged 34,525 m^3 $year^{-1}$, jumping by 5.3 fold in 2015 to a new level, presumably due to an improvement in the veracity of reporting beginning in 2015. The new level presumed to originate in the municipality of Rorainópolis (90%, see text) is close (4.5% below) to the amount authorized for sale from clearcutting projects in 2015, the only year with data on the clearcutting projects after this shift (data on clearcutting projects are available for 2010-2015). The volume data for clearcutting authorizations therefore appears to be a good representation of the portion (estimated at 90%) of volume processed by sawmills in Rorainópolis that originates within the municipality and therefore in the 520.5-km^2 area where we mapped selective logging. During the 6 years with data for authorizations of clearcutting projects (2010-2015) the mean amount authorized was 101,945.8 m^3 $year^{-1}$. From this 1.2% must be deducted for the logs that were sold from the areas that were authorized for clearcutting that were, in fact, actually clearcut (see text), meaning that the volume harvested through selective logging was 100.742.5 m^3 $year^{-1}$. If one considers that this annual harvest also applies to the preceding 4 years (2006-2009), when substantial logging activity is known to have taken place, then the harvest intensity considering the 10-year 2006-2015 period was 19.4 m^3 ha^{-1}. Considering the mean basic density the wood of 0.770 (See text Section 2.3.2), this removal in logs represents 14.9 Mg ha^{-1}. To obtain the reduction in live biomass from the selective logging we must also include the stumps and crowns of the harvested trees, as well as the biomass of unharvested trees killed from damage in the logging operations. Nogueira et al. (2008) found that stumps represented 1% of the biomass of the commercial boles in 264 harvested trees in Brazil's "arc of deforestation" in the southern part of Brazilian Amazonia. Applying this percentage, the stumps represent 0.15 Mg ha^{-1}, and the trunk from the ground to the first significant branch for the harvested trees represents 15.05 Mg ha^{-1}. Crowns were found to represent an average of 30.8% of the aboveground biomass in 121 trees in dense forest near Manaus (da Silva, 2007, p. 57). The crowns of the harvested trees therefore represent 6.7 Mg ha^{-1}, and the total (commercial log + stump + crown) represents 21.75 Mg ha^{-1}. Since this illegal selective logging does not employ reduced-impact techniques, damage equal to 64% of the harvested biomass is considered, based on studies reviewed in Fearnside (1995, p. 321). This increases the aboveground biomass loss to 35.67 Mg ha^{-1}.

Table S7. Comparison of official data sources on log volumes in Rorainópolis

Year	Volume processed in sawmills (m^3) (a)	Processed log volume assumed to come from Rorainópolis (m^3) (b)	Volume authorized in deforestation projects (m^3) (c)	Volume authorized in forest-management projects (m^3) (d)	Discrepancy between processed volume assumed to come from Rorainópolis and volume authorized in deforestation projects (m^3)	(%)
2007	40,000	36,000				
2008	32,700	29,430				
2009	32,500	29,250				
2010	33,000	29,700	133,939.0		104,239.0	351.0
2011	32,600	29,340	13,027.8		-16,312.2	-55.6
2012	35,000	31,500	150,319.5		118,819.5	377.2
2013	36,400	32,760	46,156.7		13,396.7	40.9
2014	34,000	30,600	114,311.3		83,711.3	273.6
2015	179,147	161,232	153,920.6		-7,311.7	-4.5
2016	193,210	173,889		20,066.4		
2017	424,601	382,141		14,712.8		
2018	155,942	140,348		41,789.7		
2019	170,000	153,000		13,079.7		
2020				149,611.8		
2010-2015		315,132.3	611,674.9		296,542.6	94.1
2010-2014		153,900	457,754.0		303,854.3	197.4

(a) Brazil, IBGE (2021).
(b) Assumed 90% originates from the municipality of Rorainópolis and 10% from the neighboring municipality of Caracaraí and São Luiz. Volume from indigenous areas is assumed not to be reported.
(c) Table S3.
(d) Table S4.

1.9 Selective logging

1.9.1 Mapping of the selective logging

For mapping selective logging, 16 images were used: 10 images from Landsat 5 TM and six from Landsat 8 OLI / TIRS (Table S8). The classification was checked by field observations in burned and unburned areas in 21 inventoried plots after the fires occurred (Barni et al., 2017), of which 17 were used in the present study. We also used a vector file (shapefile) provided by FEMARH for areas licensed for deforestation (128.3 km^2) in our study area during the same period of analysis (2007 to 2015) as a way to resolve doubts about spectral patterns in the images caused by SL. After mapping SL for this interval, the vector files were gathered in a single vector layer, converting this to an SL map (Figure S3).

Table S8. Mapping of selective logging (SL) from 2007 to 2015 in the study area.

*Year	Image date	**Satellite data	SL (km^2)	%	***Deforestation (km^2)	%
2007	21 Sept.	Landsat 5	39.7	6.2	19.4	11.3
2008	10 Nov.	Landsat 5	37.6	5.8	26.3	15.3
2009	29 Nov.	Landsat 5	46.9	7.3	18.2	10.6
2010	15 Oct.	Landsat 5	75.9	11.8	16.1	9.3
2011	31 Aug.	Landsat 5	80.4	12.5	11.2	6.5
2012	–	–	–	–	15.5	9.0
2013	23 Oct.	Landsat 8	72.4	11.2	22.8	13.2
2014	29 Dec.	Landsat 8	93.1	14.4	19.5	11.3
2015	30 Nov.	Landsat 8	198.7	30.8	23.3	13.5
TOTAL	16	–	644.8	100.0	172.3	100.0

***** No images were observed for the year 2012 in our study area.
** RGB and NDVI images.
*** Deforestation in the municipality of Rorainópolis (Brazil, INPE, 2020).

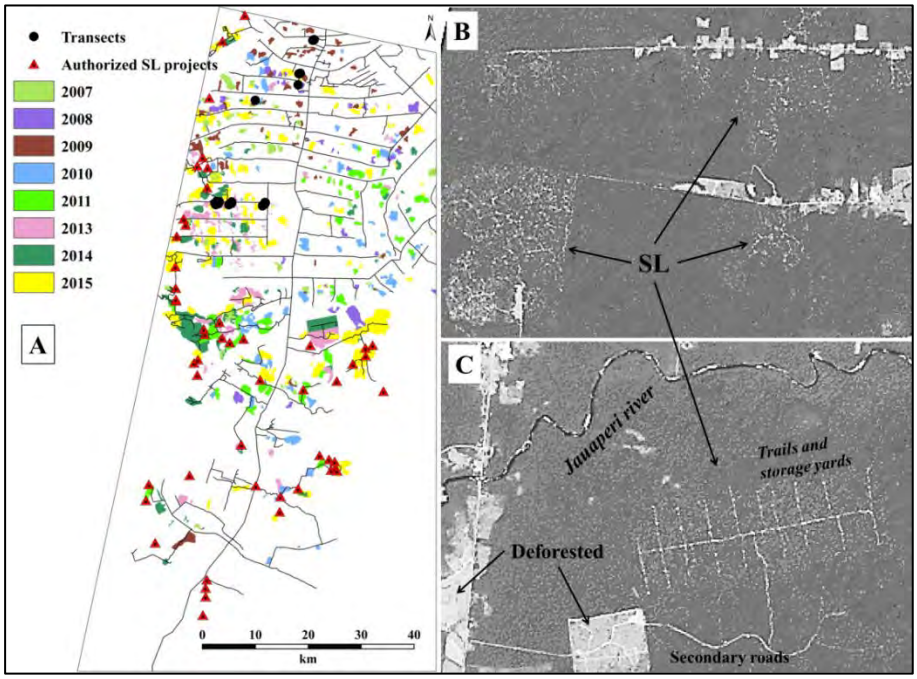

Figure S3. (A) Selective-logging map from 2007 to 2015 with the location of the 17 transects from the forest inventory and SL projects authorized by FEMARH in the study area, and in (B) and (C) detection of the SL areas in the RGB and NDVI images (Scale: 1: 50,000).

1.9.2 Severity of fire according to the year of selective logging

Analysis of the fire severity classes in areas impacted by SL showed that the class with the greatest severity ("very strong") increased with decreasing time elapsed between the harvesting of wood and the occurrence of the fire. For example, for areas logged in 2007 the difference between the "light" and "very strong" classes was 7.4%, while for areas logged in 2015 (the year the fire started in the region) this difference was ~ 3 times greater (21.9%) (Table S9).

Table S9. Severity of fire according to the year of selective logging

Year	Light Area (km^2)	%	Moderate Area (km^2)	%	Strong Area (km^2)	%	Very strong Area (km^2)	%	Total
2007	5.5	10.8	6.1	10.4	4.5	10.0	3.0	11.6	**19.1**
2008	3.3	6.4	3.0	5.2	1.9	4.2	0.8	2.9	**8.9**
2009	7.1	13.9	7.6	13.0	4.8	10.5	2.1	8.1	**21.5**
2010	6.0	11.8	5.0	8.7	2.7	6.0	0.9	3.6	**14.7**
2011	3.7	7.2	4.0	6.9	2.9	6.4	1.4	5.3	**11.9**
2013	4.7	9.3	7.4	12.7	6.8	15.1	3.9	14.8	**22.8**
2014	4.6	9.1	6.8	11.7	6.5	14.4	3.9	15.1	**21.9**
2015	16.0	31.5	18.3	31.4	15.1	33.5	10.0	38.4	**59.5**
Total	**51.0**	**100.0**	**58.2**	**100.0**	**45.2**	**100.0**	**26.1**	**100.0**	**180.5**

1.10 Calculation of weights-of-evidence

1.10.1 *A priori* probabilities of fire events

The weights-of-evidence originated from the Bayesian method of calculating conditional probabilities. Its application in modeling the dynamics of land-use and land-cover change assumes that it is possible to calculate the probability *a posteriori* of an event happening based on information obtained *a priori* from a set of conditions (evidence) that favored or determined the event in question. In our study, a set of conditions or "evidences" was transformed into maps of distance variables (maps of continuous variables) and maps of categorical variables (maps of classes) to represent influences on the occurrence of forest fires in the study area in 2015/2016 (Figure S4). The calculations of the weights-of-evidence and of the probability map were carried out in a sub-model in the Dinamica-EGO software with a stacking of the maps (Soares-Filho et al., 2014) (Figures S5 and S6).

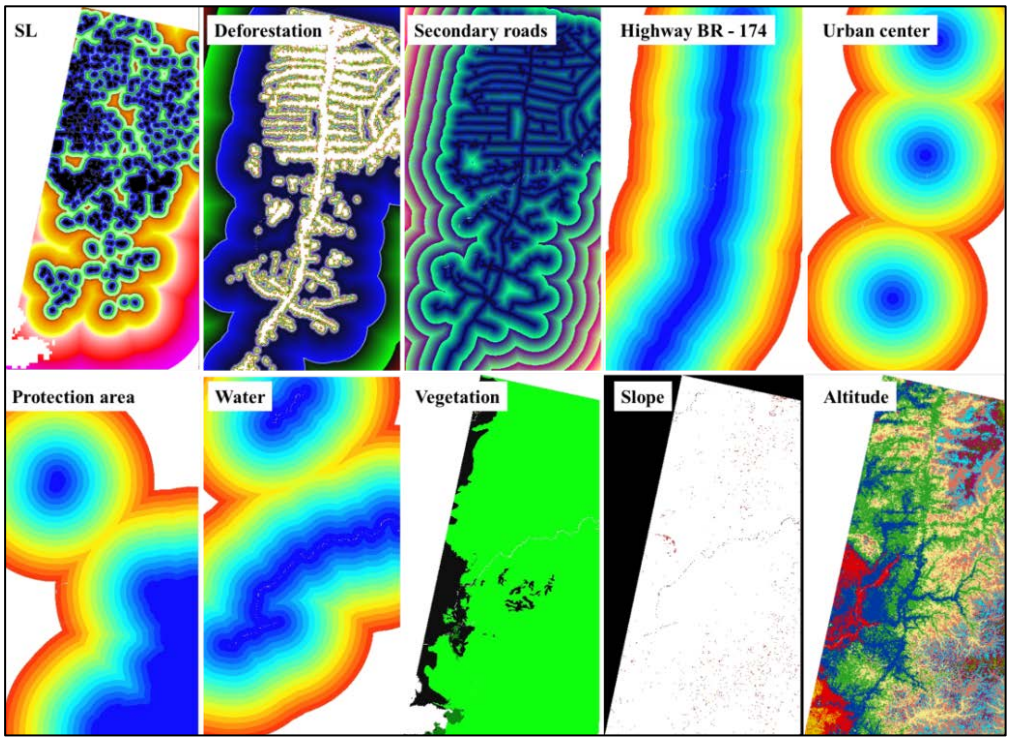

Figure S4. Set of continuous variables (with distance ranges) and categorical variables (vegetation, slope and altitude). SL = selective logging.

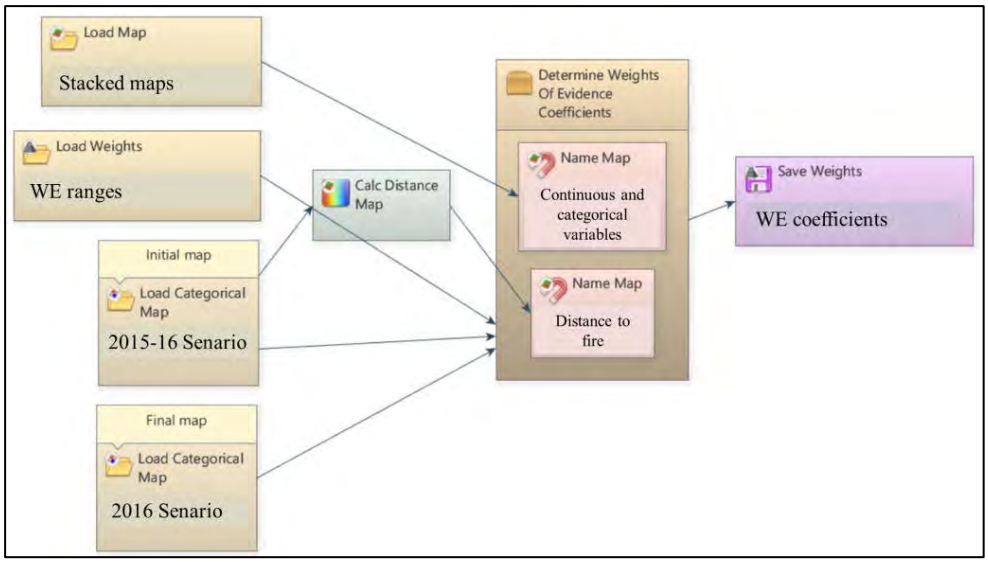

Figure S5. Submodel of the Dinamica-EGO software for calculating the weights-of-evidence coefficients. **Source**: adapted of the Dinamica-EGO guidebook (https://csr.ufmg.br/dinamica/).

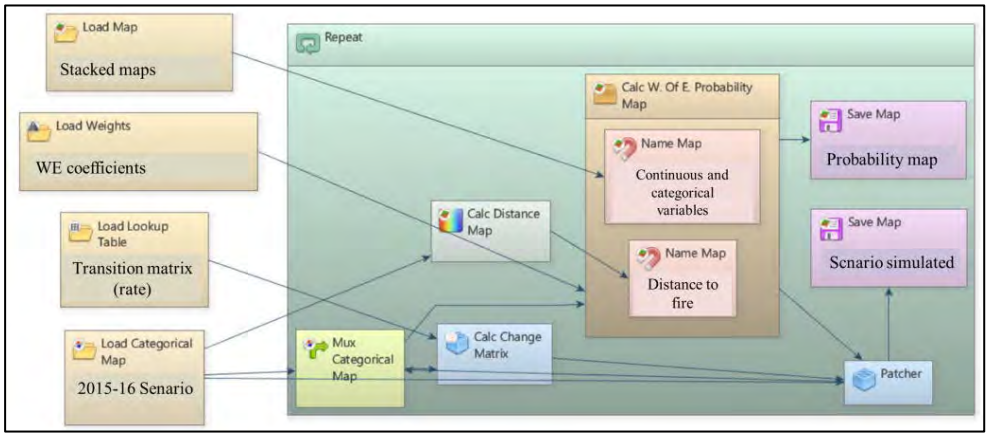

Figure S6. Submodel of the Dinamica-EGO software for calculating the map of transition probabilities and the simulated fire map. **Source**: adapted of the Dinamica-EGO guidebook (https://csr.ufmg.br/dinamica/).

The influence of the weights-of-evidence can be positive or negative. The coefficients of the weights-of-evidence are positive when they favor or promote an increase in the probability of a class transition, and they are negative when they inhibit the class transition, decreasing its probability of occurrence. For example, the spatial probability map (derived from weights-of-evidence) will indicate to the software which sets of pixels representing forest on a land-use map at time t_1 have a greater chance or probability of changing to a burnt area at time t_2. The variable "distance to secondary roads," for example, will have its maximum positive (+) weight-of-evidence in the first meters away from the fire, and at progressively greater distances this influence will decrease until it becomes negative (-), reaching its negative maximum at the most distant point.

In the modeling the weights-of-evidence represent the amount of influence of each variable on the probability of transition of a cell representing a particular state (i: forest) to change to another state (j: fire (*F*)), depending, for example, on its location within a distance range. In this way, the cell that is located closest to where the phenomenon occurred has a higher chance or greater probability. This relationship can be represented by equations (1) to (9) below, derived from the Bayesian inference method:

$$P(F/A) = \frac{P(F \cap A}{P(A)} \quad (1)$$

$$P(A/F) = \frac{P(A \cap F)}{P(F)} \quad (2)$$

$$P(A \cap F) = P(A/F) * P(F) \quad (3)$$

Likewise, considering non-event F, as not F ($\hat{F}$), we obtain (4):

$$P(\hat{F} \ / \ \mathrm{A}) = P\left(\hat{F}\right) * \frac{P(A/\hat{F})}{P(A)} \quad (4)$$

Now replacing (4) in (1), we have (5):

$$P(F/A) = P(F) * \frac{P(A/F)}{P(A)} \quad (5)$$

Applying the ratio between Equations (6) and (7), we obtain (8): (6)

$$O(F/A) = O(F) * \frac{P(A/F)}{P(A/\hat{F})} \quad (6)$$

$$\log O(F/A) = \log O(F) + \log \frac{P(A/F)}{P(A/\hat{F})} \quad (7)$$

$$\log O(F/A) = \log O(F) + W^{+} \quad (8)$$

Thus:

$$\log O(F/A) = \log O(F) + \sum_{i=1}^{n} W_i^{+} \quad (9)$$

Where “{F}” and “O {F / A}” are proportions of *a priori* probability that the “F” (fire) event occurs, and the fire event occurs given a spatial pattern “A”, respectively. “W +” is, therefore, the weight-of-evidence of event F occurring given the spatial pattern “A”. Thus, the calculation of the *a posteriori* spatial transition probability “i → j” for a spatial data set "(B, C, D, ... N)" can be represented by (10):

$$P(\mathrm{i} \rightarrow \mathrm{j}/\mathrm{B} \cap C \cap D ... \cap N) = \frac{e^{\sum W_i^{+}}}{1 + e^{\sum W_i^{+}}} \quad (10)$$

Where, "B, C, D, ..., N" are values of the k spatial variables estimated at positions "x, y", being represented by their respective weights-of-evidence "W + N". For more details on the weights-evidence method, see Barni et al. (2015).

1.10.2 Correlation between spatial variables in the calculation of weights-of-evidence

Application of the weights-of-evidence method presupposes spatial independence between variables. In the case of pairs of variables with a correlation above 0.5, one of them must be removed from the set of maps that will be used in the modeling in order to guarantee compliance with the model's assumption of independence (Bonham-Carter, 1994). This independence is

measured or estimated by observing some parameters, mainly that of contingency, which, like Pearson's correlation analysis (Figueiredo-Filho and Silva Junior, 2009), indicates the amount of correlation that exists between two spatial variables (Table S10).

Table S10. Correlated variables in the calculation of the weights of evidence.

Variable 1	Variable 2	CHI Sq.	CRAMMER	CONTING	ENTROPY	INF_C*INCERT
Deforestation	Secondary roads	26324385.8	0.38	0.86	4.36	0.35
Fire	Deforestation	13591362.2	0.31	0.81	4.97	0.20
SL	Secondary roads	11137374.0	0.30	0.78	4.75	0.21
BR-174	Village	12300562.7	0.29	0.78	4.74	0.24
Fire	SL	10654858.5	0.26	0.77	5.07	0.18
Fire	Secondary roads	10387346.3	0.29	0.77	5.04	0.18
Deforestation	SL	9312302.5	0.26	0.75	4.87	0.17
BR-174	Secondary roads	7309303.3	0.22	0.68	4.88	0.14
BR-174	Deforestation	7117818.5	0.21	0.67	4.88	0.14
Fire	Protected area	4585235.4	0.20	0.65	5.02	0.13
Fire	BR-174	5084155.0	0.20	0.65	5.22	0.09
Protected area	SL	4263722.4	0.19	0.64	4.83	0.13
Protected area	BR-174	4550167.7	0.19	0.63	4.80	0.13
Secondary roads	Village	4673617.7	0.19	0.61	5.07	0.11
Deforestation	Village	4629794.4	0.18	0.61	5.09	0.10
BR-174	SL	3819157.9	0.17	0.59	5.06	0.07
Protected area	Altitude	3321756.0	0.23	0.59	4.28	0.12
Fire	Village	3152213.0	0.14	0.57	5.35	0.07
SL	Water	2948194.9	0.15	0.56	5.14	0.06
Protected area	Secondary roads	3536961.0	0.16	0.56	4.90	0.09
Protected area	Deforestation	3378198.9	0.15	0.55	4.93	0.09
Protected area	Village	2480305.7	0.14	0.53	5.06	0.07
Protected area	Water	2553570.6	0.14	0.52	4.96	0.08
Water	Altitude	2382190.2	0.19	0.52	4.64	0.07
Altitude	Vegetation	2335823.6	0.40	0.49	2.34	0.10
Secondary roads	Altitude	2291973.7	0.18	0.49	4.60	0.06
SL	Village	2019896.1	0.12	0.48	5.23	0.06
Water	SL year class	214633.3	0.21	0.48	4.20	0.06
Village	SL year class	211868.6	0.21	0.48	4.30	0.06
Protected area	SL year class	181646.8	0.20	0.47	4.06	0.08
BR-174	Altitude	1947197.2	0.17	0.46	4.58	0.06
Fire	Water	1609818.9	0.10	0.45	5.42	0.04
Deforestation	Water	2167922.4	0.11	0.45	5.25	0.05
Deforestation	Altitude	1804270.1	0.16	0.44	4.61	0.05
BR-174	SL year class	168417.7	0.18	0.44	4.18	0.05
Fire	Altitude	1596435.5	0.15	0.43	4.85	0.04
SL	Altitude	1589559.1	0.15	0.42	4.64	0.04
BR-174	Water	1463864.6	0.10	0.40	5.25	0.03
Fire	SL year class	133323.5	0.16	0.40	4.38	0.05
Village	Altitude	1239948.2	0.13	0.39	4.74	0.04
Water	Secondary roads	1464261.7	0.10	0.38	5.29	0.04
Deforestation	SL year class	111350.3	0.15	0.37	4.21	0.04
Water	Village	1102794.6	0.07	0.36	5.38	0.03
Water	Vegetation	771589.5	0.25	0.33	3.11	0.04

BR-174	Vegetation	798968.3	0.24	0.32	2.98	0.04
Slope	Altitude	838470.5	0.11	0.32	4.11	0.03
Protected area	Vegetation	654567.6	0.23	0.31	2.79	0.03
Secondary roads	SL year class	68851.5	0.12	0.30	3.87	0.02
SL year class	Altitude	68036.6	0.12	0.29	3.69	0.03
Secondary roads	Vegetation	475077.7	0.18	0.25	3.01	0.02
Village	Vegetation	440054.3	0.18	0.25	3.13	0.02
SL	Vegetation	444832.3	0.18	0.24	3.05	0.02
Deforestation	Vegetation	327915.6	0.15	0.21	3.00	0.02
Fire	Vegetation	323501.9	0.15	0.21	3.26	0.01
SL year class	Vegetation	26428.0	0.14	0.19	2.18	0.02
Protected area	Slope	221586.4	0.06	0.18	4.52	0.01
Water	Slope	203287.6	0.06	0.17	4.76	0.01
SL	Slope	154153.7	0.05	0.14	4.74	0.00
Secondary roads	Slope	145011.5	0.05	0.14	4.69	0.00
Deforestation	Slope	128456.0	0.04	0.13	4.68	0.00
BR-174	Slope	123456.6	0.04	0.13	4.66	0.00
Fire	Slope	91464.5	0.04	0.11	4.94	0.00
Slope	Vegetation	54819.5	0.06	0.09	2.46	0.00
Village	Slope	29033.2	0.02	0.06	4.80	0.00
SL year class	Slope	2855.3	0.02	0.06	3.98	0.00
SL	SL year class	0.0	0.00	0.00	1.93	0.00

SL = Selective logging

1.11 Model validation using an exponential decay function and fuzzy similarity

The "Calc reciprocal similarity map" function in Dinamica-EGO calculates a two-way similarity from the first map (simulated scenario) to the second (initial scenario) and from the second to the third (final scenario) (Figure S7). It is advisable to always chose the smaller similarity value since random maps tend to produce artificially high fits when compared univocally, because they spread the changes over the entire map. This test employs an exponential decay function truncated outside of a window size of 11 × 11 cells. The test result is returned in a .csv table file (Figure S8).

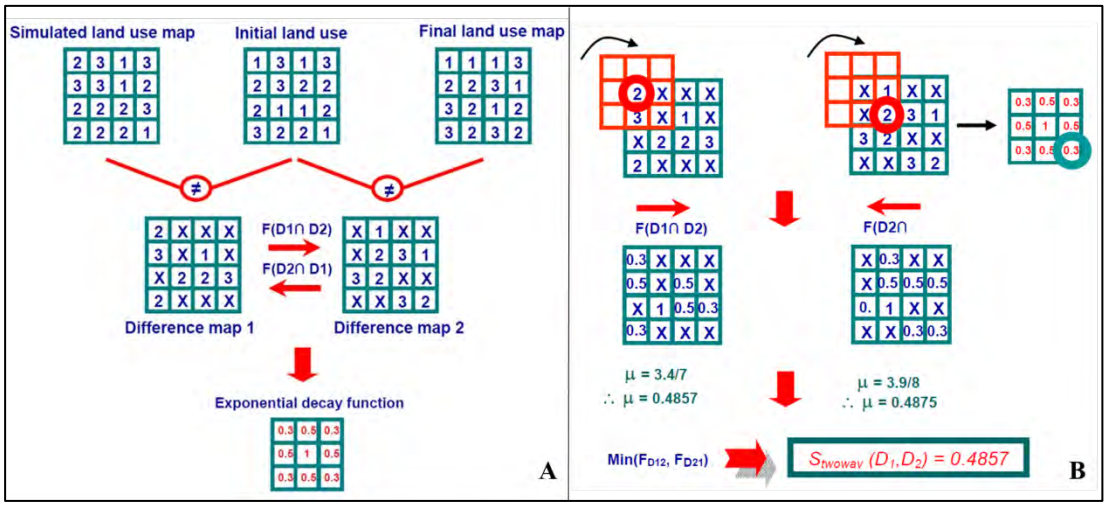

Figure S7. Fuzzy comparison method using a map of differences and an exponential decay function. The process applies a constant decay function in which all window weights are set to 1 (**A**). The window convolutes over the map, obtaining a fuzzy value for the central cell (**B**). X = null values in the map. **Source**: adapted from the Dinamica-EGO guidebook (https://csr.ufmg.br/dinamica/).

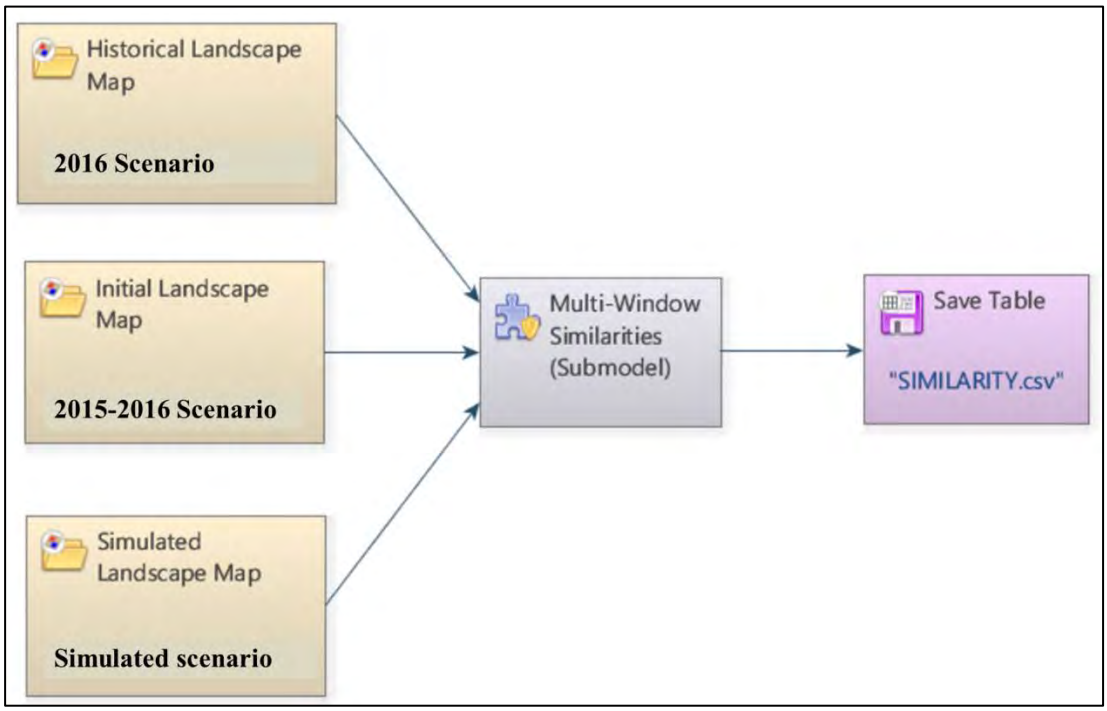

Figure S8. Submodel for similarity calculation in Dinamica-EGO software. **Source**: adapted from the Dinamica-EGO guidebook (https://csr.ufmg.br/dinamica/).

2. Results

2.1 Areas of occurrence

The areas of occurrence of the main variables distributed in the study area are presented in Table S11. The original forest area was estimated at 6512.4 km^2, representing 97.8% of the study area.

Table S11. Original forest area (km^2), protected areas, non-forest and deforestation occurring in the study area.

	Class	Area (km^2)	%	Forest fire (km^2)	Forest fire % of forest area	SL-fire (km^2)	SL-fire % of forest fire area	SL (km^2)	SL-fire (%) of SL area
Original vegetation	**Forest**	6,512.4	97.8						
	Non-forest	144.9	2.2						
	Total	**6,657.3**	**100.0**						
2016 vegetation	**Forest**	5,410.3	81.3	682.2	12.6	180.7	26.5	644.8	28.0
	Deforestation	1,102.1	16.6	-	-	-	-	-	-
	Non-forest	144.9	2.2	-	-	-	-	-	-
	Total	**6,657.3**	**100.0**						
Protected areas	**Indigenous land**	875.6	13.2	0.0	0.0	-	-	-	-
	Anauá National Forest	2.6	0.04	2.0	76.9	-	-	-	-

2.2 Estimates of biomass by forest type

Dense ombrophilous forest was the most affected by understory fires, totaling 532.7 km^2 and the estimated affected dry biomass at the time of the fire totaling 26.2 × 10^6 Mg. Ecotone forest had the smallest area (9.3 km^2) and the smallest amount (0.3 × 10^6 Mg) of affected biomass (Table S12).

Table S12. Estimated biomass before and after logging in the area affected by fire separated by forest type and by selective-logging status.

	Original biomass (prior to logging)				Affected biomass (biomass at time of fire)					
Forest	**Total area affected bv fire (km^2)**	**Total biomass in area affected bv fire (10^6 Mg)**	**% of total biomass in area affected by fire**	**Mean original biomass (Mg ha^{-1})**	**Area W/SL (km^2)**	**Biomass after logging (10^6 Mg)**	**Biomass removed or killed by SL (10^6 Mg)**	**Affected biomass in area with SL (10^6 Mg)**	**Area Wo/SL (km^2)**	**Affected biomass in area Wo/SL (10^6 Mg)**
Campinarana	140.0	3.6	13.2	255.6	28.3	0.71	0.1	0.7	111.7	2.9
Ecotone	9.3	0.33	1.2	360.3	0.0	0.0	0.0	0.0	9.3	0.3
Ombrophilous	532.7	23.2	85.6	435.3	152.3	6.63	0.5	6.1	380.3	16.6
Total	**681.9**	**27.1**	**100**	**397.4**	**180.62**	**7.34**	**0.6**	**6.7**	**501.3**	**19.8**

The estimation of forest biomass was performed for each forest type separately for areas with and without selective logging (SL). The dense ombrophilous forest (Ds) had the largest extension in terms of occupied area (87.8%) and in terms of biomass (92.5%) in relation to the total biomass (277.37 × 10^6 Mg) estimated for the original forest areas. The biomass of the areas under SL (27.6× 10^6 Mg) represented 9.9% of the total biomass found in the study area, and 95.3% of that biomass was under dense ombrophilous forest (Table S13).

Table S13. Estimated biomass (Mg) in the study area separated by areas affected by selective logging (SL) (W-SL) and areas not affected by SL (Wo-SL).

Type	**Area (km^2)**	**%**	**Biomass (10^6 Mg)**	**Mean (Mg ha^{-1})**	Wo/**SL 10^6 Mg)**	**%**	**W/SL (10^6 Mg)**	**%**
Campinarana	727.9	11.2	18.7	256.3	17.4	93.0	1.30	7.0
Ecotone	63.7	1.0	2.1	335.5	2.1	99.1	0.02	0.9
Ombrophilous	5,720.8	87.8	256.7	448.5	230.3	89.7	26.3	10.3
Total	**6,512.4**	**100.0**	**277.4**	**425.9**	**249.8**	**90.0**	**27.6**	**9.9**

Wo/SL = without selective logging. W-SL = with selective logging.

The cumulative loss of original biomass by deforestation up to 2016 was estimated at 48.04 × 10^6 Mg, representing more than twice (2.1 times) the biomass affected by SL in our study area. The area deforested in dense ombrophilous forest (1059.3 km^2) represented 96.1% of the total area deforested by 2016 and 97.5% of the total biomass lost (Table S14).

Table S14. Biomass lost due to cumulative deforestation up to 2016.

Deforestation	**Area (km^2)**	**%**	**Biomass (10^6 Mg)**	**%**	**Mean (Mg ha^{-1})**
Campinarana	33.8	3.1	0.9	1.8	255.6
Ecotone	8.8	0.8	0.3	0.7	367.4
Ombrophilous	1,059.3	96.1	46.9	97.5	442.3
Total	**1,101.9**	**100.0**	**48.0**	**100.0**	**436.0**

2.3 Vulnerability of the forest to understory fires in SL areas

SL influenced the spread of fire in the study area during the 2015/2016 El Niño event within the fire-severity classes. Based on NDVI image analyses, the graphs in Figure S9 show positive correlations between fires and the logging practiced in years immediately prior to the fires.

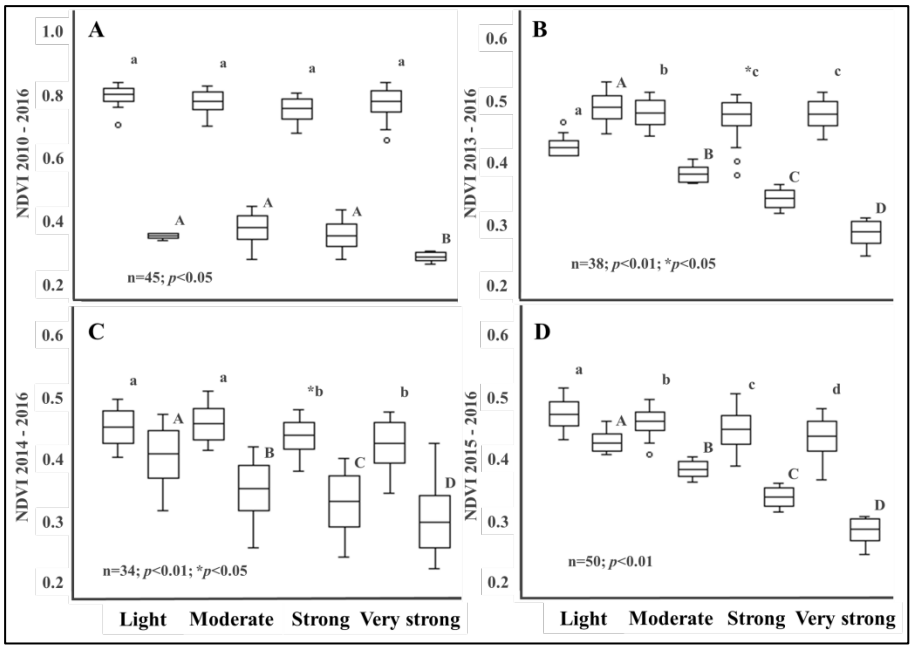

Figure S9. Comparison between NDVI values in SL areas in years prior to the fires with the NDVI values in the fire image for 2016. (A) Comparison of NDVI values between the years 2010 and 2016. (B) Comparison of NDVI values between the years 2013 and 2016. (C) Comparison of NDVI values between the years 2014 and 2016 and (D) comparison of NDVI values between the years 2015 and 2016. The lower-case letters above the boxes indicate statistical results between the NDVI values in years prior to the fires considering the fire-severity classes of the fires, while upper-case letters indicate the statistical results for the NDVI values in the 2016 image at the fire-event locations, also considering the severity classes.

2.4 Fire and SL behavior as a function of forest-edge distance

The highest occurrence of forest fires (114.9 km^2: 20.1%) in the study area was found in the range between 0 to 120 m from the forest edge. The SL presented a similar result reaching 113.9 km^2 (24.3%) in the first interval. The burned areas affected by SL were calculated at 161.2 km^2 in the range between 0 and 1200 m, representing 89.4% of the total reached in the study area (Table S15).

Table S15. Fire and SL occurrence depending on the distance from the forest edge.

Range (m)	Fire (km^2)	%	SL (km^2)	%	SL x Fire (km^2)	%	SL / Fire (%)	SL x Fire / Fire (%)	SL x Fire / SL (%)
0 -- 120	114.9	20.1	113.9	24.3	23.7	14.7	99.1	20.6	20.8
120 -- 240	95.3	16.7	58.2	12.4	25.3	15.7	61.1	26.5	43.4
240 -- 360	77.8	13.6	55.2	11.8	23.5	14.6	70.9	30.2	42.5
360 -- 480	68.8	12.0	52.8	11.3	21.2	13.2	76.7	30.9	40.2
480 -- 600	55.6	9.7	47.5	10.1	17.9	11.1	85.3	32.2	37.7
600 -- 720	43.6	7.6	38.1	8.1	14.1	8.7	87.2	32.3	37.0
720 -- 840	37.8	6.6	32.5	6.9	11.8	7.3	85.9	31.2	36.3
840 -- 960	31.7	5.6	28.4	6.1	9.9	6.1	89.5	31.0	34.7
960 -- 1080	25.3	4.4	23.0	4.9	7.7	4.7	91.2	30.3	33.2
1080 -- 1200	21.0	3.7	19.3	4.1	6.3	3.9	92.2	30.1	32.7
Total	**571.7**	**100.0**	**468.8**	**100.0**	**161.2**	**100.0**			
Percent	**682.2**	**83.8**	**644.8**	**72.7**	**180.4**	**89.4**			

2.5 Model-validation results

The results of the validation test are shown in Figure S10. The model containing all variables showed the greatest similarity between the observed and simulated scenarios.

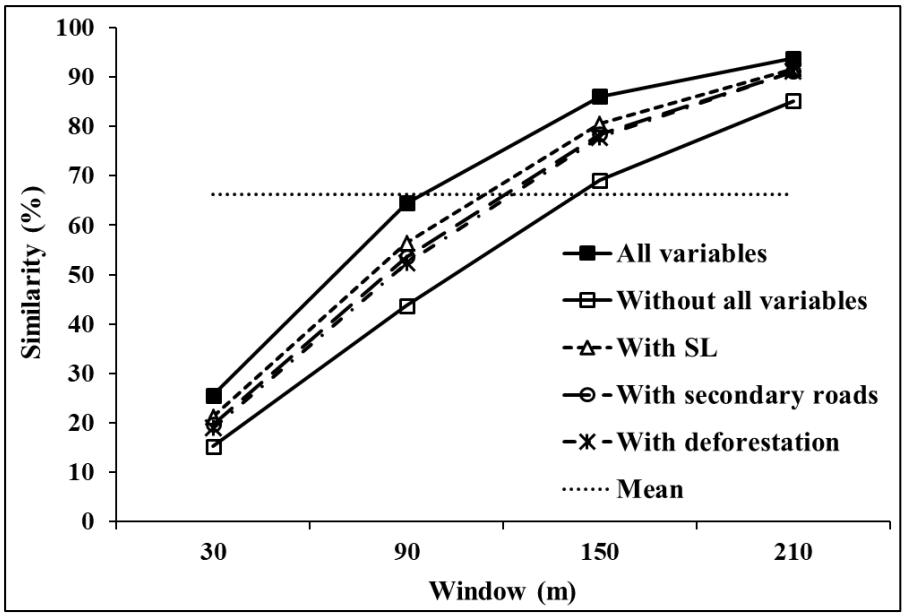

Figure S10. Similarity test between the modeled maps and the fire map for 2016.

2.6 Forest vulnerability to fire

The assessment of the vulnerability maps showed that the SL influenced the spread of fire in the study area during the 2015/2016 El Niño event. The exposure of forest areas to fires increased by 366.2% in the most-vulnerable range, which ranged from 79.11 to 99.99% (0.7911 to 0.9999 probability), with the presence of SL areas in the model compared to the absence of SL in the model (Table S16; Figures S11 and S12).

Table S16. Classes of vulnerability of the forest to forest fires.

	Whole area regardless of impacts		**Without SL**		**Without secondary roads**		**Without deforestation**	
Range	**Area (km^2)**	**%**	**Area (km^2)**	**%**	**Area (km^2)**	**%**	**Area (km^2)**	**%**
0.0004 - 0.1488	2,550.4	47.1	1,750.1	32.3	2,467.7	45.6	2,478.5	45.8
0.1489 - 0.3955	421.4	7.8	822.4	15.2	511.3	9.4	501.1	9.3
0.3956 - 0.6109	407.5	7.5	938.9	17.3	500.3	9.2	478.1	8.8
0.6110 - 0.7910	547.7	10.1	1,315.5	24.3	588.7	10.9	609.0	11.2
0.7911 - 0.9999	1,487.9	27.5	587.9	10.9	1,346.7	24.9	1,348.1	24.9
Total	**5,414.8**	**100.0**	**5,414.8**	**100.0**	**5,414.8**	**100.0**	**5,414.8**	100.0
	Without SL, roads or deforestation		**With SL**		**With secondary roads**		**With deforestation**	
Range	**Area (km^2)**	**%**	**Area (km^2)**	**%**	**Area (km^2)**	**%**	**Area (km^2)**	**%**
0.0004 - 0.1488	1,576.3	29.1	1,859.3	34.3	1,557.9	28.8	1,497.2	27.7
0.1488 - 0.3955	784.3	14.5	821.7	15.2	966.9	17.9	985.9	18.2
0.3956 - 0.6109	694.7	12.8	671.2	12.4	707.8	13.1	802.0	14.8
0.6110 - 0.7910	2,045.3	37.8	912.2	16.8	735.8	13.6	951.1	17.6
0.7911 - 0.9999	314.2	5.8	1,150.4	21.2	1,446.4	26.7	1,178.6	21.8
Total	**5,414.8**	**100.0**	**5,414.8**	**100.0**	**5,414.8**	**99.9**	**5,414.8**	100.0

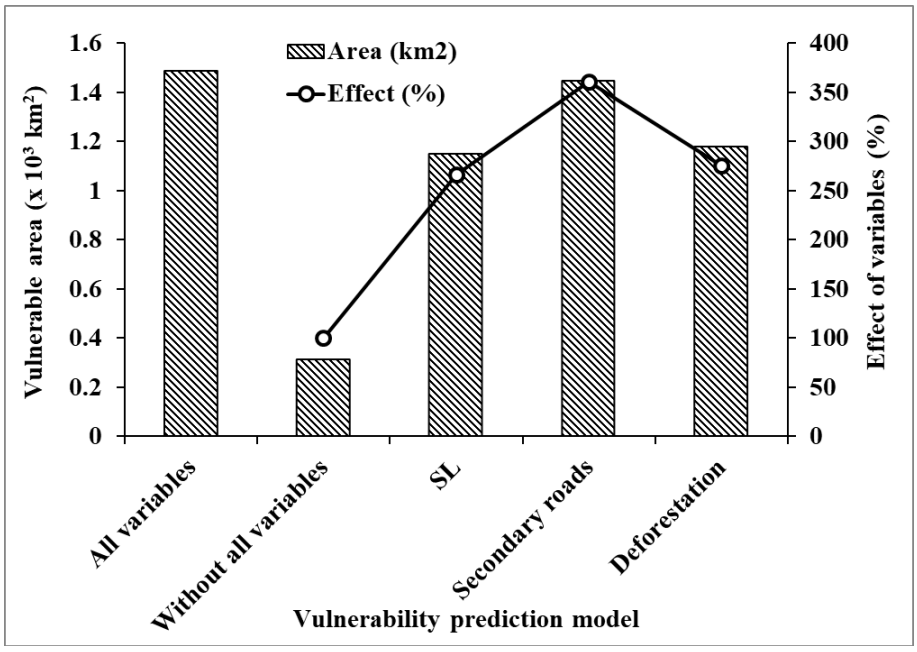

Figure S11. Area vulnerable to understory forest fires in the study area.

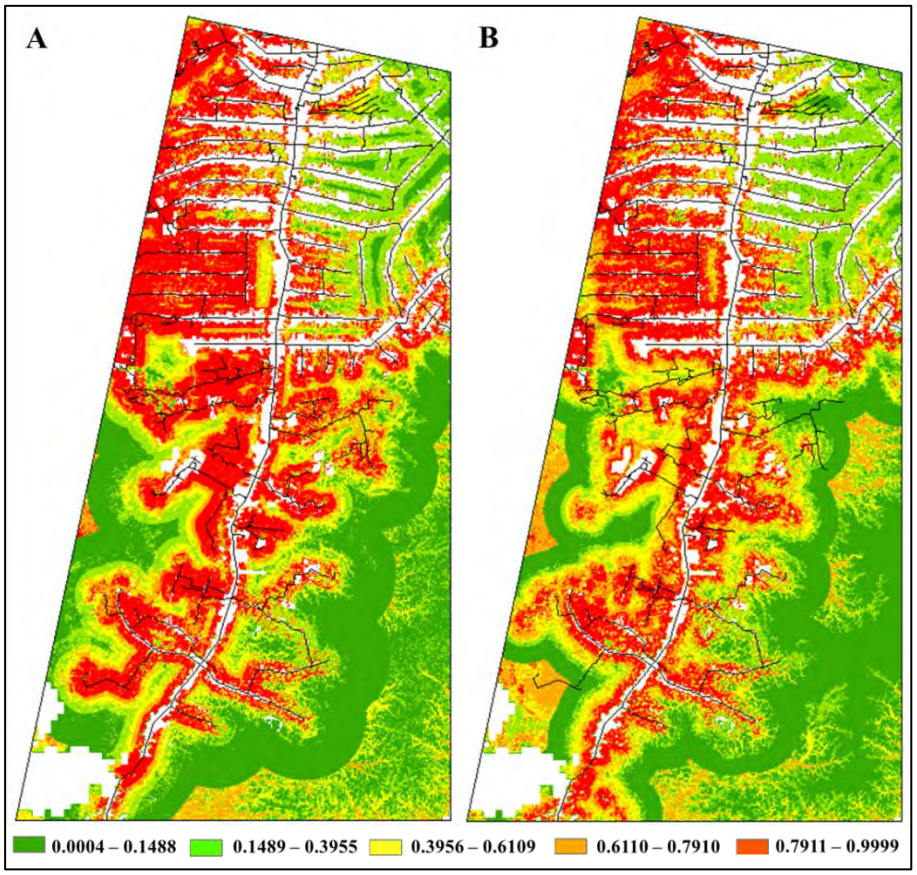

Figure S12. Maps of the vulnerability of the forest to understory fires. (A) forest-vulnerability map calculated from variables not correlated with "secondary roads," plus the "secondary roads" variable and (B) forest-vulnerability map calculated from variables not correlated with "deforestation," plus the "deforestation" variable. The legend below the figure shows the ranges of probability ([0.1]) of the forest being affected by fire.

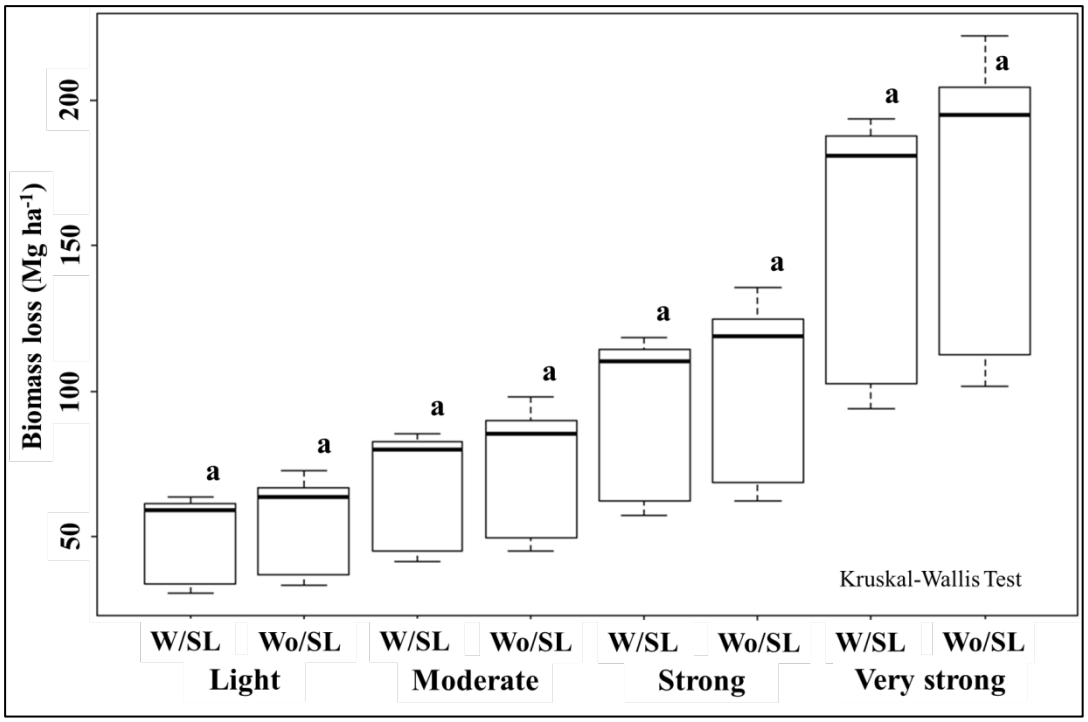

Figure S-13. Biomass loss (Mg ha^{-1}) by fire-severity class in areas with SL (W/SL) and areas without SL (Wo/SL) considering all forest types in the study area. The lower-case letters above the boxes indicate that there was no significant difference ($p < 0.05$) between the loss of biomass by fire in previously logged areas and unlogged areas within each severity class.

References

Barni, P.E., Fearnside, P.M., Graça, P.M.L.A., 2015. Simulating deforestation and carbon loss in Amazonia: impacts in Brazil's Roraima state from reconstructing Highway BR-319 (Manaus-Porto Velho). Environmental Management, 55, 124–1138. http://rd.springer.com/article/10.1007%2Fs00267-015-0447-7

Barni, P.E., Silva, E.B.R., Silva, F.C.F., 2017. Incêndios florestais de sub-bosque na zona de florestas úmidas do sul de Roraima: Área atingida e biomassa morta. In: Anais do Simpósio Brasileiro de Sensoriamento Remoto 2017. Campinas, SP, Brazil: Galoá, pp. 6280-6287. Available at: https://bityl.co/5JeV. Accessed on: 21 November 2020.

Bonham-Carter, G., 1994. Geographic Information Systems for Geoscientists: Modeling with GIS. Pergamon, New York, USA. 398 pp.

Brazil, IBGE (Instituto Brasileiro de Geografia e Estatística), 2021. Produção da Extração Vegetal e da Silvicultura: Tabela289. Available at: https://sidra.ibge.gov.br/Tabela/289. Accessed on: 19 March 2021.

Brazil, INPE (Instituto Nacional de Pesquisas Espaciais), 2020. Projeto PRODES – Monitoramento da Floresta Amazônica por Satélite. São José dos Campos, SP, Brazil: INPE. Available at: https://bityl.co/5JeS. Accessed on: 21November 2020.

da Silva, R.P., 2007. Alometria, Estoque e Dinâmica da Biomassa de Florestas Primárias e Secundárias na Região de Manaus (AM). Ph.D. Thesis in tropical forest science, Instituto Nacional de Pesquisas da Amazônia (INPA), Manaus, Amazonas, Brazil. https://repositorio.inpa.gov.br/bitstream/1/4966/1/Roseana_Silva.pdf

Fearnside, P.M., 1995. Global warming response options in Brazil's forest sector: Comparison of project-level costs and benefits. Biomass and Bioenergy, 8(5), 309-322. https://doi.org/10.1016/0961-9534(95)00024-0

Fearnside, P.M., 1997. Wood density for estimating forest biomass in Brazilian Amazonia. Forest Ecology and Management, 90(1), 59-89. https://doi.org/10.1016/S0378-1127(96)03840-6

Figueiredo Filho, D.B., Silva Junior, J.A., 2009. Desvendando os mistérios do coeficiente de correlação de Pearson (r). Política Hoje, 18(1), 115-146. https://periodicos.ufpe.br/revistas/politicahoje/article/view/3852/3156

Higuchi, N., Santos, J., Ribeiro, R.J., Minette L., Biot, Y., 1998. Biomassa da parte aérea da vegetação da floresta tropical úmida de terra-firme da Amazônia brasileira. Acta Amazonica, 28(2), 153-166. https://doi.org/10.1590/1809-43921998282166

Nogueira, E.M., Nelson, B.W., Fearnside, P.M., 2005. Wood density in dense forest in central Amazonia, Brazil. Forest Ecology and Management, 208(1-3), 261-286. https://doi.org/10.1016/j.foreco.2004.12.007

Nogueira, E.M., Fearnside, P.M., Nelson, B.W., Barbosa, R.I., Keizer, E.W.H., 2008. Estimates of forest biomass in the Brazilian Amazon: New allometric equations and adjustments to biomass from wood-volume inventories. Forest Ecology and Management, 256(11), 1853-1857. https://doi.org/10.1016/j.foreco.2008.07.022

Saldarriaga, J.G., West, D.C., Tharp, M., Uhl, C., 1988. Long-term chronosequence of forest succession in the upper Rio Negro of Colombia and Venezuela. Journal of Ecology,76, 938–958. https://doi.org/10.2307/2260625

Silveira, L.H.C., Rezende, A.V., Vale, A.T., 2013. Teor de umidade e densidade básica da madeira de nove espécies comerciais amazônicas. Acta Amazonica, 43(2), 179–184. https://doi.org/10.1590/S0044-59672013000200007

Soares-Filho, B.S., Ferreira, B.M., Filgueira, D.S., Rodrigues, H.O., Hissa, L.B.V., Lima, L.S., Machado, R.F., Costa, W.L.S., 2014. Dinamica project. Remote Sensing Center. Federal University of Minas Gerais (UFMG), Belo Horizonte, Minas Gerais, Brazil. Available at: http://www.csr.ufmg.br/dinamica/. Last access: 12 June 2020.